



Calhoun: The NPS Institutional Archive
DSpace Repository

Theses and Dissertations

1. Thesis and Dissertation Collection, all items

1991

Enhancement of boiling heat transfer in di-electric fluids.

Egger, Robert A.

<http://hdl.handle.net/10945/28168>

This publication is a work of the U.S. Government as defined in Title 17, United States Code, Section 101. Copyright protection is not available for this work in the United States.

Downloaded from NPS Archive: Calhoun



Calhoun is the Naval Postgraduate School's public access digital repository for research materials and institutional publications created by the NPS community. Calhoun is named for Professor of Mathematics Guy K. Calhoun, NPS's first appointed -- and published -- scholarly author.

Dudley Knox Library / Naval Postgraduate School
411 Dyer Road / 1 University Circle
Monterey, California USA 93943

<http://www.nps.edu/library>

NAVAL POSTGRADUATE SCHOOL

Monterey , California



THESIS

ENHANCEMENT OF BOILING HEAT TRANSFER
IN DI-ELECTRIC FLUIDS

by

Robert A. Egger

September 1991

Thesis Advisor

M.D. Kelleher

Approved for public release; distribution is unlimited

T259716

Unclassified

Security classification of this page

REPORT DOCUMENTATION PAGE

Report Security Classification Unclassified			1b Restrictive Markings		
Security Classification Authority			3 Distribution/Availability of Report		
Declassification/Downgrading Schedule			Approved for public release; distribution is unlimited.		
Performing Organization Report Number(s)			5 Monitoring Organization Report Number(s)		
Name of Performing Organization Naval Postgraduate School		6b Office Symbol (if applicable) 34	7a Name of Monitoring Organization Naval Postgraduate School		
Address (city, state, and ZIP code) Monterey, CA 93943-5000			7b Address (city, state, and ZIP code) Monterey, CA 93943-5000		
Name of Funding/Sponsoring Organization		8b Office Symbol (if applicable)	9 Procurement Instrument Identification Number		
Address (city, state, and ZIP code)			10 Source of Funding Numbers		
			Program Element No	Project No	Task No
			Work Unit Accession No		
Title (Include security classification) ENHANCEMENT OF BOILING HEAT TRANSFER IN DI-ELECTRIC FLUIDS					
Personal Author(s) Robert A. Egger					
Type of Report Master's Thesis		13b Time Covered From To		14 Date of Report (year, month, day) September 1991	15 Page Count 94
Supplementary Notation The views expressed in this thesis are those of the author and do not reflect the official policy or position of the Department of Defense or the U.S. Government.					
Cosati Codes			18 Subject Terms (continue on reverse if necessary and identify by block number)		
Id	Group	Subgroup	word processing, Script, GML, text processing.		
Abstract (continue on reverse if necessary and identify by block number)					
<p>Direct application of two-phase heat transfer in the liquid cooling of electronic components in fluorinated hydrocarbons (FC-72), is severely inhibited by the excessive amount of superheat required to initiate nucleate boiling. To conduct an experimental study of nucleate pool boiling of FC-72, an experimental test chamber was constructed. This chamber utilized five horizontal platinum wires of 0.05 mm diameter spaced 2.0 cm vertically from each other. The lowest wire was progressively heated from the natural convection region through nucleate boiling, and a study was made on the effects of the boiling wake time on the heat transfer rate of the upper wires.</p>					
Distribution/Availability of Abstract Unclassified/unlimited <input type="checkbox"/> same as report <input type="checkbox"/> DTIC users			21 Abstract Security Classification Unclassified		
Name of Responsible Individual D. Kelleher			22b Telephone (include Area code) (408) 646-2530		22c Office Symbol ME/Kk

FORM 1473,84 MAR

83 APR edition may be used until exhausted
All other editions are obsolete

security classification of this page

Unclassified

Approved for public release; distribution is unlimited.

Enhancement of Boiling Heat Transfer
in Di-Electric Fluids

by

Robert A. Egger
Lieutenant , United States Navy
B.E. Mechanical Engineering, Cleveland State University, 1985

Submitted in partial fulfillment of the
requirements for the degrees of

MASTER OF SCIENCE IN MECHANICAL ENGINEERING
and
MECHANICAL ENGINEER

from the

NAVAL POSTGRADUATE SCHOOL
September 1991

ABSTRACT

Direct application of two-phase heat transfer in the liquid cooling of electronic components in fluorinated hydrocarbons (FC-72), is severely inhibited by the excessive amount of superheat required to initiate nucleate boiling. To conduct an experimental study of nucleate pool boiling of FC-72, an experimental test chamber was constructed. This chamber utilized five horizontal platinum wires of 0.05 mm diameter spaced 2.0 cm vertically from each other. The lowest wire was progressively heated from the natural convection region through nucleate boiling, and a study was made on the effects of the boiling wake plume on the heat transfer rate of the upper wires.

C-2000
C.1

TABLE OF CONTENTS

I. INTRODUCTION	1
A. HISTORICAL	1
B. BACKGROUND	1
C. PREVIOUS WORK	2
D. OBJECTIVES	4
II. EXPERIMENTAL APPARATUS	5
A. DESCRIPTION OF COMPONENTS	5
1. Test Chamber	5
2. Aluminum Cover Plate	6
3. Heaters	6
4. Thermocouples	6
5. Insert Board	6
B. INSTRUMENTATION	7
1. Platinum Wire	7
2. Power Supplies	8
3. Acquisition Unit	8
III. EXPERIMENTAL PROCEDURE	17
A. PREPARATIONS	17
1. Normal Warm-Up Procedure	17
2. Post Warm-up Procedure	17
B. DATA ACQUISITION PROCEDURE	18
C. DATA REDUCTION	18
1. Numerical Data	18
2. Fluid Property Data	20
IV. RESULTS AND DISCUSSION	22
A. INDIVIDUALLY POWERED WIRES	22
1. Natural Convection	22
2. Nucleate Boiling	23

3. Departure from Nucleate Boiling	23
B. BUBBLE PUMPING EFFECT ON HEAT TRANSFER RATE	32
1. Passive Wire at Low Heat Flux	32
2. Passive Wire at Medium Heat Flux	33
3. Passive Wire at High Heat Flux	33
4. Wire 1 Passive with Wire 2 varying	34
5. Subcooled	34
V. CONCLUSIONS	44
A. SINGLE WIRE BOILING	44
B. PASSIVE WIRE ANALYSIS	44
APPENDIX A. CALIBRATION	46
A. PLATINUM WIRE	46
1. Surface Micro-Structure	46
2. Desirability for Using Platinum	48
B. BACKGROUND	48
C. INITIAL CALIBRATION	48
1. Calibration Heating Bath	49
2. Temperature Measurements	49
3. Resistance Measurements	49
4. Calibration Procedure	49
D. IN PLACE CALIBRATION	50
1. Inplace Calibration Procedure.	50
E. CALIBRATION RESULTS	50
1. Platinum Wire 1	50
2. Platinum Wire 2	51
3. Platinum Wire 3	51
4. Platinum Wire 4	51
5. Platinum Wire 5	52
F. SUMMARY	63
APPENDIX B. SAMPLE CALCULATIONS	65
A. DETERMINATION OF DERIVED VALUES	65
1. Determination of the Average Bulk Temperature	65

2. Determination of Wire Current	65
B. DETERMINATION OF PLATINUM WIRE RESISTANCE	65
1. Determination of Wire Surface Temperature	65
2. Determination of Input Power	66
3. Determination of Heat Flux	66
C. DETERMINATION OF FLUID PROPERTIES	66
1. Film Temperature	66
2. Thermal Conductivity	67
3. Liquid Density	67
4. Kinematic Viscosity	67
5. Specific Heat	67
6. Thermal Expansion Coefficient	68
7. Thermal Diffusivity	68
8. Prandlt Number	68
APPENDIX C. UNCERTAINTY ANALYSIS	69
A. UNCERTAINTY IN SURFACE AREA	69
B. UNCERTAINTY IN POWER	70
C. UNCERTAINTY IN HEAT FLUX	71
D. UNCERTAINTY IN TEMPERATURE	71
E. UNCERTAINTY OF WIRE SURFACE TEMPERATURE	71
APPENDIX D. DATA ACQUISITION PROGRAMS USED	74
A. PLATINUM WIRE RESISTANCE CALIBRATION PROGRAM	74
B. MAIN DATA ACQUISITION PROGRAM	76
C. NUSSELT EVALUATION PROGRAM	79
LIST OF REFERENCES	81
INITIAL DISTRIBUTION LIST	83

LIST OF TABLES

Table 1.	MEASURED RESISTANCE VALUES FOR 2 OHM RESISTORS	7
Table 2.	PLATINUM WIRE PHYSICAL PARAMETERS FOR EQUATION (3.4) AND EQUATION	19
Table 3.	INDIVIDUAL WIRE RUNS	22
Table 4.	DATA POINT DESCRIPTION	32

LIST OF FIGURES

Figure 1.	Power consumption vs Volume	2
Figure 2.	Overall experimental setup	9
Figure 3.	Experimental Chamber in Detail	10
Figure 4.	Side View of Experimental Apparatus	11
Figure 5.	Rear View of Experimental Chamber	12
Figure 6.	Insert Board	13
Figure 7.	schematic Drawing of Insert Board	14
Figure 8.	Isometric View of Apparatus	15
Figure 9.	Condensor Surface Details	16
Figure 10.	Wire1 boiling curve	24
Figure 11.	Wire 1 Boiling Curves over time	25
Figure 12.	Wire 1 boiling curve	26
Figure 13.	Wire 1 Boiling Curve	27
Figure 14.	Wire 2 boiling curve	28
Figure 15.	Wire 3 Boiling Curve	29
Figure 16.	Wire 4 boiling curve	30
Figure 17.	Overlay of previous curves	31
Figure 18.	Wire 2 at 8500 W/	35
Figure 19.	Wire 4 at 8500 W/	36
Figure 20.	Wire 2 at 20,500 W/	37
Figure 21.	Wire 4 at 20,500 W/	38
Figure 22.	Wire 2 at 40,000 W/	39
Figure 23.	Wire 4 at 35,000 W/	40
Figure 24.	Wire 1 passive, Wire 2 active	41
Figure 25.	Wire 2 at 35,000 W/	42
Figure 26.	Wire 2 at 53,000 W/	43
Figure 27.	Surface micro geometry	46
Figure 28.	Surface micro geometry	47
Figure 29.	Surface micro geometry	47
Figure 30.	Thermocouple Uncertainty	53
Figure 31.	Calibration of Platinum Wire 1	54

Figure 32. Calibration of Platinum Wire 1 55

Figure 33. Calibration of Platinum Wire 2 56

Figure 34. Calibration of Platinum Wire 2 57

Figure 35. Calibration of Platinum Wire 3 58

Figure 36. Calibration of Platinum Wire 3 59

Figure 37. Calibration of Platinum Wire 4 60

Figure 38. Calibration of Platinum Wire 4 61

Figure 39. Calibration of Platinum Wire 5 62

Figure 40. Calibration of Platinum Wire 5 63

NOMENCLATURE

<i>Symbols</i>	<i>Units</i>	<i>Description</i>
A	m^2	Surface Area of Test Surface
β	$1/^\circ K$	Thermal Expansion Coefficient
C_p	J/kg	Fluid's Specific Heat
D	m	Wire Diameter
g	m/sec^2	Acceleration due to gravity
h	$W/m^2 \cdot ^\circ K$	Heat Transfer Coefficient
k	$W/m \cdot ^\circ K$	Thermal Conductivity
L	m	Wire Lengths
Q	W	Heat Transfer
q	W/m^2	Heat Flux
R	ohms	Resistance
T	$^\circ K$	Temperature
Ra	ND	Rayleigh Number
Pr	ND	Prandlt Number
Nu	ND	Nusselt Number

SUBSCRIPTS

l	liquid
v	vapor
sat	Saturation Conditions
sub	Subcooled Conditions
bulk	Bulk Fluid Conditions
PtWire	Platinum Wire
Res	2Ω Resistor
surf	Surface

GREEK SYMBOLS

μ	Ns/m^2	Dynamic Viscosity
ν	m^2/s	Kinematic Viscosity
σ	N/m	Surface Tension
ρ	kg/m^3	Fluid Density
ω		Uncertainty in measurements.

I. INTRODUCTION

A. HISTORICAL

Ever since the development of the first practical solid state integrated circuit in 1959, there has been a continuous emphasis on packaging an ever higher density of logic circuits on a single substrate. Corresponding with this increase packaging density is an increasing power dissipation requirement along with an increase difficulty in the thermal management capabilities. Initially, thermal management techniques consisted of nothing more than a heat sink and natural convection air cooling. This naturally progressed into heat sinks with forced convection air cooling, and with the construction of large mainframe computers and first generation super-computers the use of indirect liquid cooling was initiated. The next practical method for heat removal is direct liquid cooling or immersion cooling of microelectronic components using dielectric liquids.

Although direct liquid cooling has been successfully employed for nearly 40 years in large hi-powered microwave equipment, klystron tubes, travelling-wave guide tubes, and power transistors [Ref. 1 : p.12], only recently has it been employed for use in the thermal management of microelectronics. The first computer systems to successfully employ immersion cooling of microelectronics were the CRAY-2 and the ETA-10 supercomputer [Ref. 2 : p. 8]. Today the research in direct immersion cooling is continuing with particular emphasis on utilizing dielectric liquids as a cooling medium, in particular the prefluorinated FC liquid family of the 3M corporation [Ref. 3].

B. BACKGROUND

The advantages offered by direct immersion cooling is self evident from Figure 1. By utilizing forced convection direct liquid cooling with FC-77, the CRAY-2 has been able to reduce it's required volume by an order of magnitude as compared to it's indirect liquid cooled competitors. This was being achieved in the CRAY-2 while at the same time maintaining the same power dissipation of the competition, [Ref. 1].

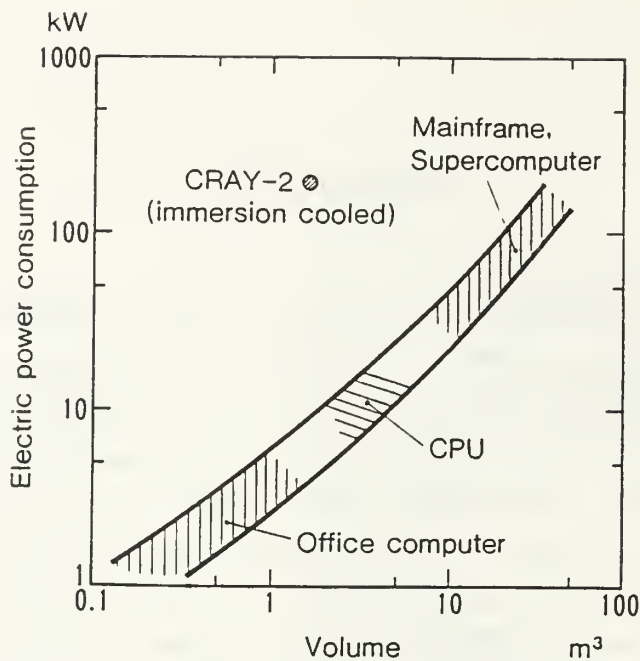


Figure 1. Power consumption vs Volume: Of present computers

As previously stated, the CRAY-2's packaging density was achievable due to direct liquid immersion cooling, however, it did use a forced convection cooling scheme. A thermal management scheme that relies on boiling heat transfer would provide an even more efficient heat transfer capability, and has been the attention of considerable research in recent years. Unfortunately, these prefluorinated dielectric fluids possess anomalies which have held back their widespread use and acceptance of direct immersion cooling.

In comparison to water and many other coolants, these prefluorinated dielectric liquids possess a lower value for their thermal conductivity, and heat of vaporization, they also have an extremely small surface tension which translates into a near zero wetting angle and therefore, a high wettability on most surfaces. This last feature results in the elimination of many potential nucleation sites which in turn results in an incipience super heat excursion which results in a very high wall temperature.

In this study, heat transfer enhancement, and therefore a surface temperature reduction, due to bubble pumping in FC-72 will be investigated.

C. PREVIOUS WORK

An extensive amount of research has been conducted in the boiling regime of dielectric liquids. The most helpful of the literature used will be noted.

You, Simon and Bar-Cohen [Ref. 4 and Ref. 5] conducted an analyses on the effects of pressure, subcooling, and dissolved gas content on the boiling heat transfer, and the boiling incipience of dielectric fluids. In their experiment they used FC-72 as the working fluid and a $0.1\mu\text{m}$ thin film of platinum on a 0.51mm diameter quartz cylinder, with the platinum film acting as both heater and temperature sensor. They concluded that:

1. An increase in pressure of 56kPa reduces wall superheat by approximately 3°C in the fully developed nucleate boiling region.
2. Subcooling has little effect on the fully developed nucleate boiling region.
3. Nucleate boiling hysteresis is observed for both the subcooled and gas-saturated cases. The hysteresis decreases as the gas content increases.
4. Incipience bubble radius computed for FC-72 was $0.05\text{-}0.1\mu\text{m}$.
5. Effects of dissolved gases in the fluid is seen at low content values as an increase in run to run variability.
6. The effect of subcooling on pool boiling incipience is apparently small.
7. A wide variation in incipience superheat values for nominally identical runs were observed.

You, Simon, Bar-Cohen and Tong [Ref. 6] conducted an experimental investigation of boiling in R-113. The experiment was conducted using 0.13mm diameter Chromel wires and 0.51mm diameter platinum thin film heater. The following was found.

1. A Scanning Electron Microscope (SEM) analysis was conducted on the surface of the thin film heater, in which the chromel wire surface was found to contain a higher density of nucleation sites compared to the thin film platinum heater.
2. The platinum heater surface was found to have a higher incipience superheat than the chromel wires, 73°C versus 38°C maximum. This tends to correlate well with item 1.
3. Again, a wide variation in incipience superheat values for nominally identical runs were experience.

Marto and Lepere [Ref. 7] conducted experiments with surface enhancements for improving pool boiling performance. Marto and Lepere using FC-72 and R-113 as working fluids compared the performance of three commercially available boiling enhancement surfaces to plain copper tubing. In each case the enhanced surface resulted in a lower wall surface temperature compared to the plain copper tube. However, the required incipience superheat for nucleation remained unaltered.

Bergles and Kim [Ref. 2] analyzed methods to reduce the temperature overshoot of immersion cooling. Their method used an active bubble generator in the fluid located

below the simulated micro chip. They used the bubble generator to activate dormant and extinct nucleation sites. They obtained a reduction of incipience superheat required from 22-33° C to 8-12° C in a working fluid of R-113.

Maddox and Mudawar [Ref. 8] studied the effect of subcooling and surface augmentation on values of Critical Heat Flux (CHF). They found that the CHF of FC-72 can achieve a level greater than 360 Watts/cm² with combined use of subcooling and surface augmentation.

Danielson, Tousignat and Bar-Cohen [Ref. 9] conducted an analysis of a large number of commercially available prefluorinated inert fluids. The method of investigation used a 0.25mm diameter platinum wire heating element, with the working fluid at saturation conditions. Important points reported are:

1. The critical heat flux of FC-72 was reported as approximately 20.3 Watts/cm².
2. The nucleate boiling characteristic of highly wetting fluids can be predicted using correlations developed for water and other fluids, but are highly dependent of the heating surface condition.
3. Single phase convection data are predicted accurately by a correlation developed by Kuehn and Goldstein.[Ref. 10]
4. The superheat excursion at incipience boiling always appears, but the magnitude varies widely.
5. The apparent radii of nucleation bubbles were calculated to be 0.1 to 0.2 μ m.

Kuehn and Goldstein [Ref. 10] has obtained a correlation of natural convective heat transfer for infinite cylinders. This correlation was used in this thesis data analysis due to the low rayleigh numbers obtained in the experimental runs.

From the 3M Product Manual [Ref. 3] it can be found that the highly wetting dielectric fluids have a high solubility for gases. FC-72 can contain up to 48% air by volume compared to 1.9% air for water. This is the necessity of thoroughly degassing the fluid prior to the experimental runs.

D. OBJECTIVES

The objective of this work was to investigate the effects of the boiling wake from a heated wire upon the heat transfer rate from wires placed within the wake. This work was carried out using the dielectric fluid FC-72.

II. EXPERIMENTAL APPARATUS

A. DESCRIPTION OF COMPONENTS

The experimental apparatus used in this study is a redesign of an experimental apparatus used in a previous thesis. Emphasize on this design was to minimize systematic errors, minimize uncertainty, and to correct deficiencies to ensure an overall increase in the data's creditability over the previous apparatus, [Ref. 11].

In Figure 2 an overall view of the experimental setup is shown, identifying all major components that were utilized. Figure 3 is a photograph of the actual experimental chamber.

The apparatus chamber consists of a box constructed of 0.75 inch thick polycarbonate sheets with a 0.25 inch thick aluminum coverplate fitted with a rubber O-Ring seal. Inside the box are two bulk heaters to raise the fluid to saturation temperature for degassing purposes, and to maintain the bulk fluid temperature near constant. The aluminum cover plate is mounted with three thermo-electric coolers, and serves as a condenser, where by the vapor condenses and returns to the chamber by gravity. An insert board is held in the chamber on which are mounted the test wires, tension springs, thermocouples, and voltage pickoffs.

1. Test Chamber

The interior dimensions of the chamber are 6.0 inches wide, by 2.375 deep, by 6.25 inches high, as shown in the isometric view of Figure 8. The entire chamber was assembled using IPN #16 Acrylic bonding adhesive and a bead of Di-Metheryl Ethelene was used to seal all seams along the interior surface to ensure liquid tightness.

To permit access for instrumentation and power leads, and as a means to ensure pressure equalization, a 0.75 inch diameter and 0.25 inch diameter hole were placed into the rear face of the chamber at the lower right and upper right corner respectively, as shown in Figure 4. Mounted securely around these access holes are lengths of tygon tubing of approximately 18 inches in length, with the opened ends suspended well above the chamber.

On the interior side walls, slots are milled to permit the placement and removal of an instrumented wire board on which the experiments are conducted. Figure 6 is a photograph of the insert board, while a schematic drawing is shown in Figure 7.

2. Aluminum Cover Plate

A 0.25 inch thick by 7.00 inch long by 3.25 inch wide aluminum plate was utilized for use as a cover plate for the chamber, and as a condenser surface for the FC-72 vapor. Mounted on the interior face are two thermocouples to monitor the condensor surface temperature, as shown in Figure 9. On the exterior face of the plate, three thermo electric coolers were installed for heat removal. To ensure a proper seal between the aluminum plate and the box structure , a shallow O-Ring groove was machined into the interior face and an O-Ring of 0.0624 inch diameter was installed. To adequately secure the cover plate to the chamber box, eight stainless steel screws of 1/16 inch diameter are used to compress the O-Ring against its mating surface.

As mentioned previously, three solid state thermoelectric cooling devices from the MELCOR corp were employed to cool the cover plate condensor. They were nominally operated about the 0.4 amps and 2.0 volts operating point, from [Ref 12] their operation curves and technical data is available.

3. Heaters

As a means of degassing the FC-72 liquid and for bulk temperature control, two strip heaters of 125mm x 11 mm were employed. These strip heaters were secured to the bottom interior surface of the chamber with epoxy, and were orientated lengthwise in the chamber such that one heater strip will be in front of and one heater strip behind the insert board. To raise the bulk fluid temperature to saturation temperature and for degassing purposed, both heaters are on line and operated at 1.8 amps and 20 volts. Once degassing is complete, the forward strip heater is electrically isolated and the rear heater is run at 0.9 amps and 20 volts. This will maintain the forward portion of experimental chamber at near saturation temperature with minimum stratification of fluid, and maintain liquid in a degassed state since the fluid is still boiling from the heater strip's surface.

4. Thermocouples

A total of Six copper-constantan type thermocouples with a wire diameter of 0.05 inches (0.127 mm) were utilized for temperature measurements. Two thermocouples were bonded to the underside of the aluminum condensor plate utilizing OMEGA Bond type 101 thermally conductive epoxy, four thermocouples were installed on the insert board, and one was used for measuring the ambient air temperature.

5. Insert Board

An insert board was designed to mount into two 0.250 inch wide grooves that were milled into the chamber side walls. Onto this insert board are mounted four

thermocouples to measure bulk fluid temperature, five platinum wires of nominally 0.002 inch (0.05mm) diameter by 4.0 inch long for conducting the actual boiling experiments. Five springs are used to maintain the platinum wire tension so no sagging develops due to thermal expansion of the wires. In Appendix A the platinum wire calibrations and specifications are shown in detail.

B. INSTRUMENTATION

In the design and assembly of this experimental apparatus, five channels were wired and instrumentation provided to measure voltage drops at select points. Each of these channels had a 2.0 ohm precision resistor wired in series with the platinum wire, where the voltage drop across the resistor was used to obtain the current flow through the platinum wire. The voltage drop measured across the platinum wire is used to obtain the wire resistance, power dissipated and the heat flux of the platinum wire. The platinum wire temperature is obtained from its resistance vs temperature calibration curve obtained prior to experimental runs. Instrumentation was additionally used to obtain the bulk fluid temperature, which will be required for calculating fluid properties.

1. Platinum Wire

Each of the five platinum wires were run in series with a 2 ohm ($\pm 1\%$) precision resistor of 25 watt power rating. The following table gives the platinum wire and resistor combinations which were used.

Table 1. MEASURED RESISTANCE VALUES FOR 2 OHM RESISTORS

Wire Channel	Measured Resistance, 20 Sample average	20 Sample Std. Dev.
1	1.9994 Ω	0.0009 Ω
2	2.0076 Ω	0.0005 Ω
3	1.9998 Ω	0.0003 Ω
4	2.0018 Ω	0.0013 Ω
5	2.0025 Ω	0.0008 Ω

A 2.0 ohm precision resistor was chosen over the previous design's 0.1 ohms precision resistor in order to reduce the calculated currents uncertainty, and there by reduce the calculated platinum wire temperature uncertainty, [Ref. 11: p. 25].

2. Power Supplies

The following power supplies were utilized and their primary function listed.

1. Hewlett Packard 6214C 0-10volts/0-1 amps: Used to power the thermal electric coolers.
2. Hewlett Packard 6214C 1-10volts / 0-1 amps: Used to power the constant heat flux platinum wire.
3. WP711 0-40 volts / 0-1 amps : Used to power the varying heat flux platinum wire.
4. Hewlett Packard 6286A 0-20volts / 0-10 amps : Used to power Heater Strips for degassing and bulk temperature maintenance.
5. Hewlett Packard 6289A 0-40 volts / 0-1.5 amps : Used to power an auxiliary illumination system or an augmenting cooling fan for the thermal electric coolers.

3. Acquisition Unit

To obtain the necessary measurements, a Hewlett Packard 3852A Data Acquisition System was employed, utilizing a Hewlett Packard 300 series desktop computer. The HP3852A utilized the following utility modules inserted into it's chassis.

1. Hewlett Packard Model 44701A Digital Integrating Voltmeter
2. Hewlett Packard Model 44705A 20 channel relay multiplexer for measuring required voltage drops.
3. Hewlett Packard Model 44713A 24 channel relay multiplexer with electronic cold junction for direct conversion of thermal couple emf to temperature.

The HP300 desktop computer was used to control the HP3852A Data acquisition system. Additionally, through specifically written programs, the computer can accomplish the required data reductions, (See Appendix D).

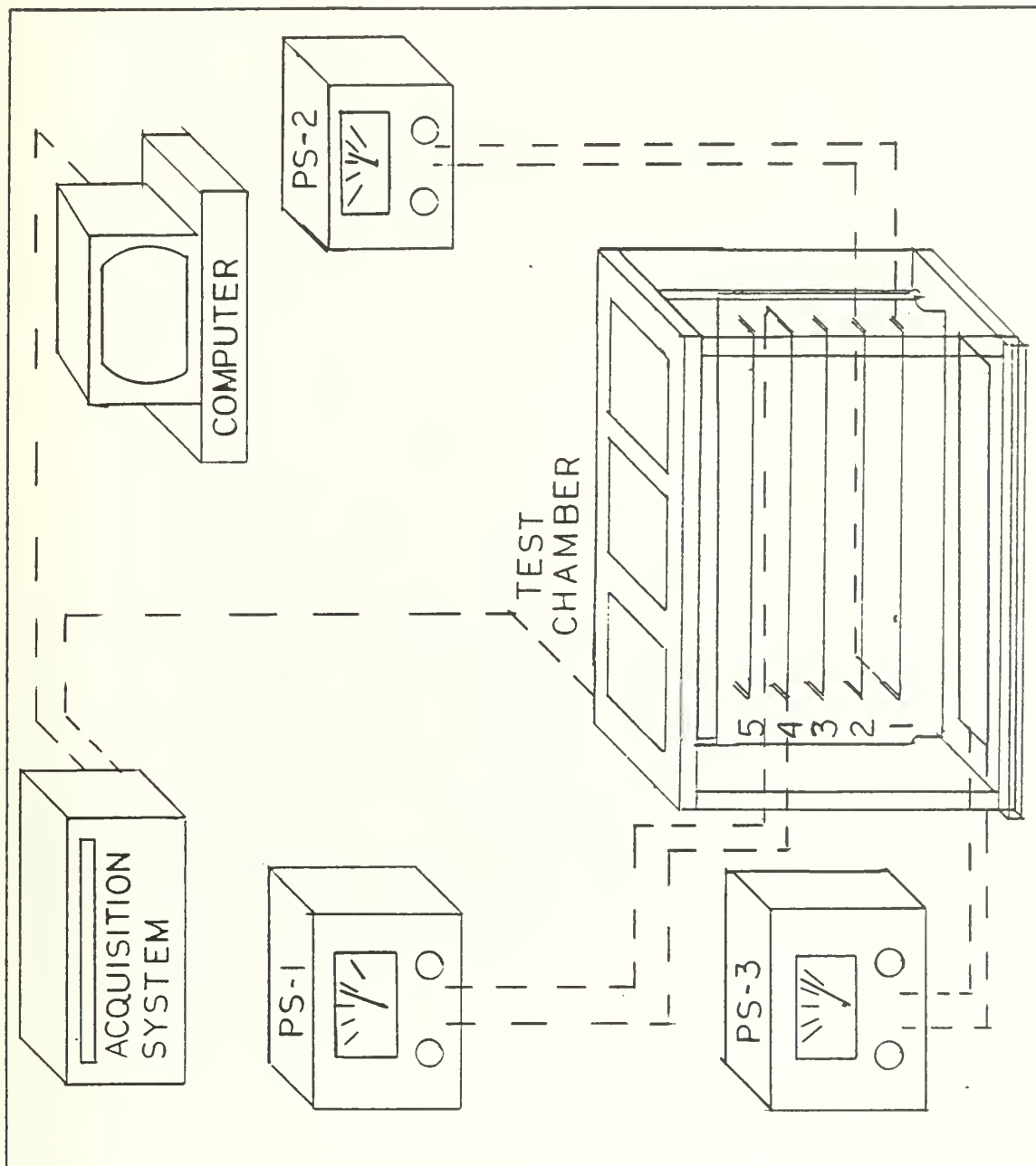


Figure 2. Overall experimental setup



Figure 3. Experimental Chamber in Detail



Figure 4. Side View of Experimental Apparatus

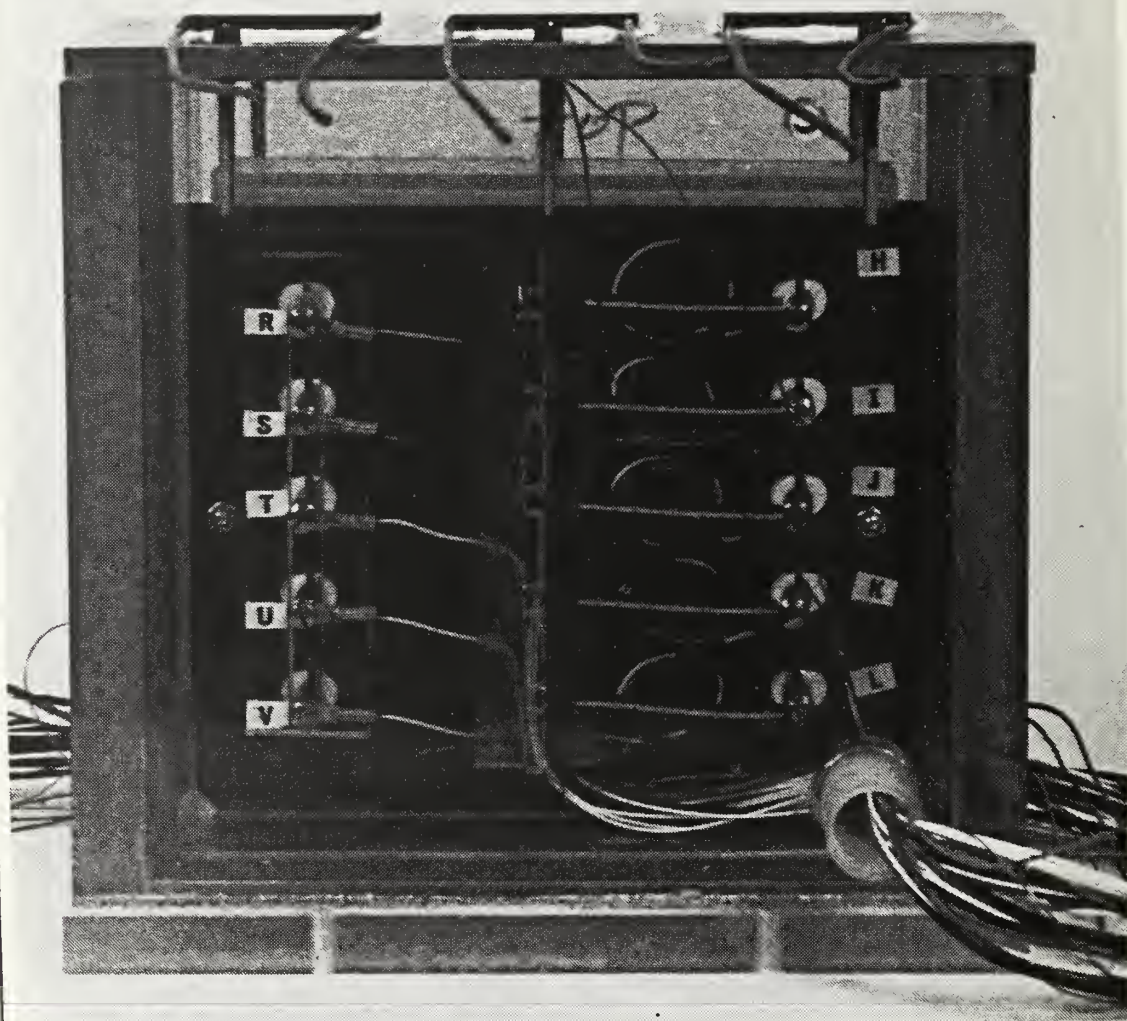


Figure 5. Rear View of Experimental Chamber

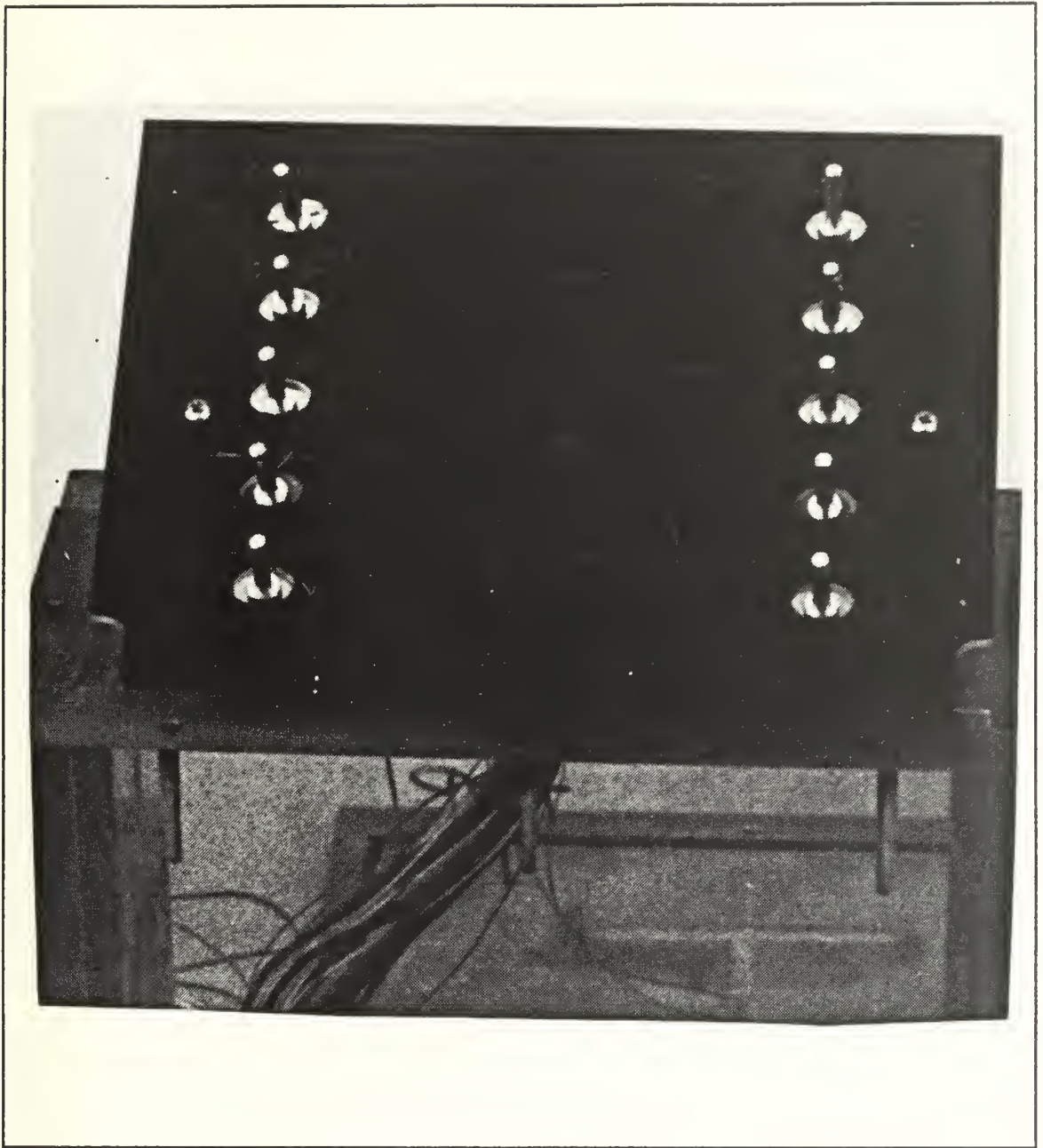


Figure 6. Insert Board

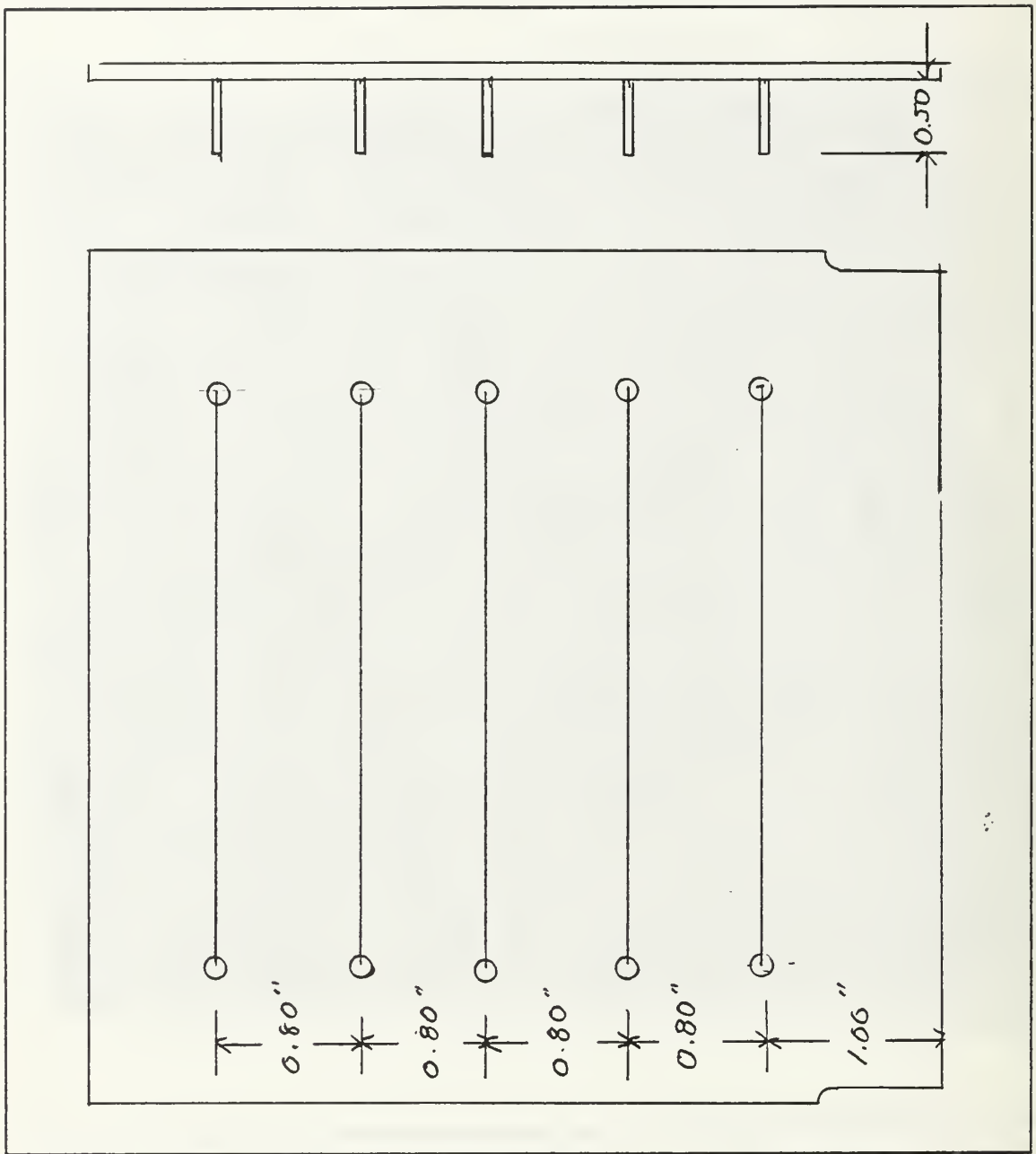


Figure 7. schematic Drawing of Insert Board

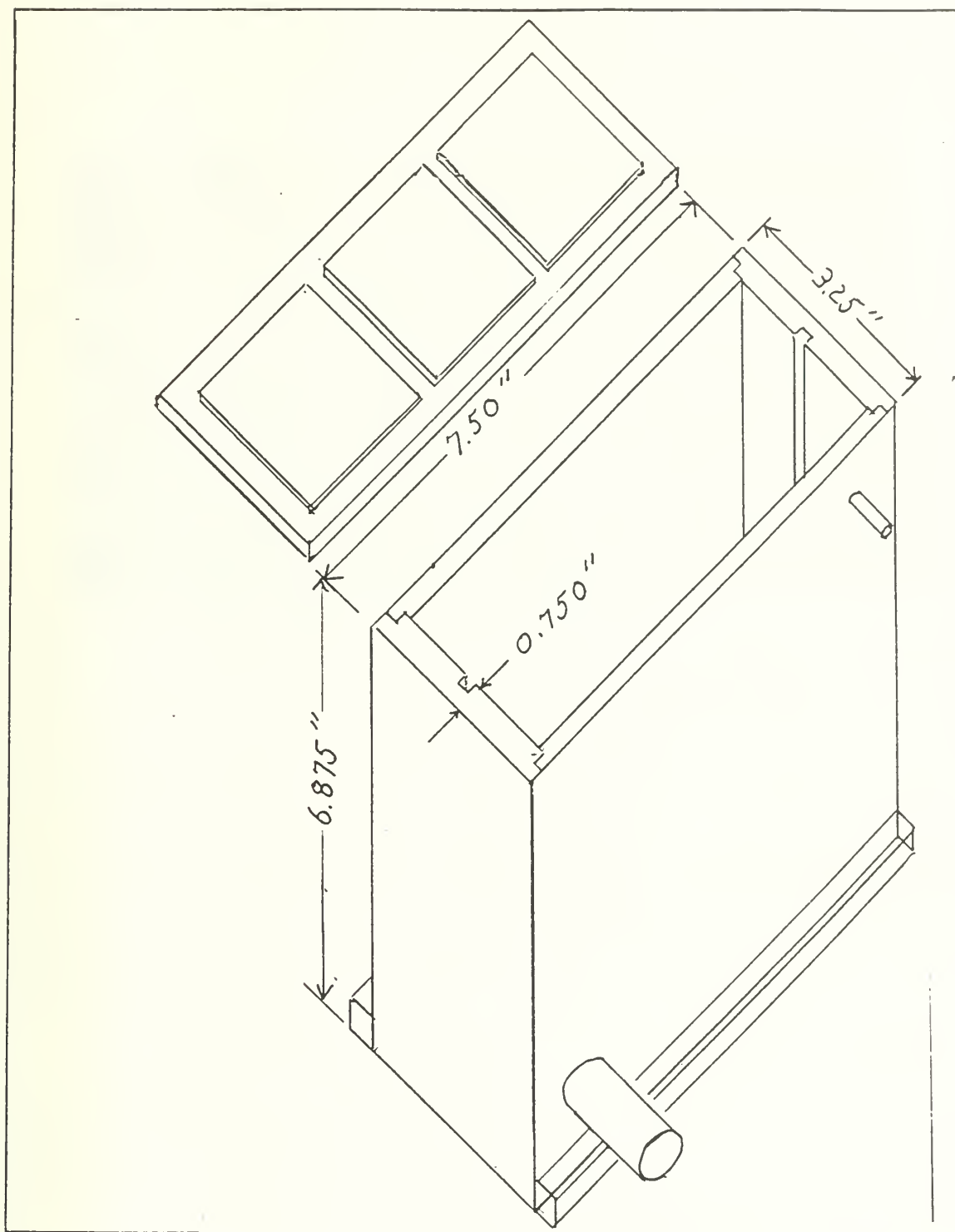


Figure 8. Isometric View of Apparatus

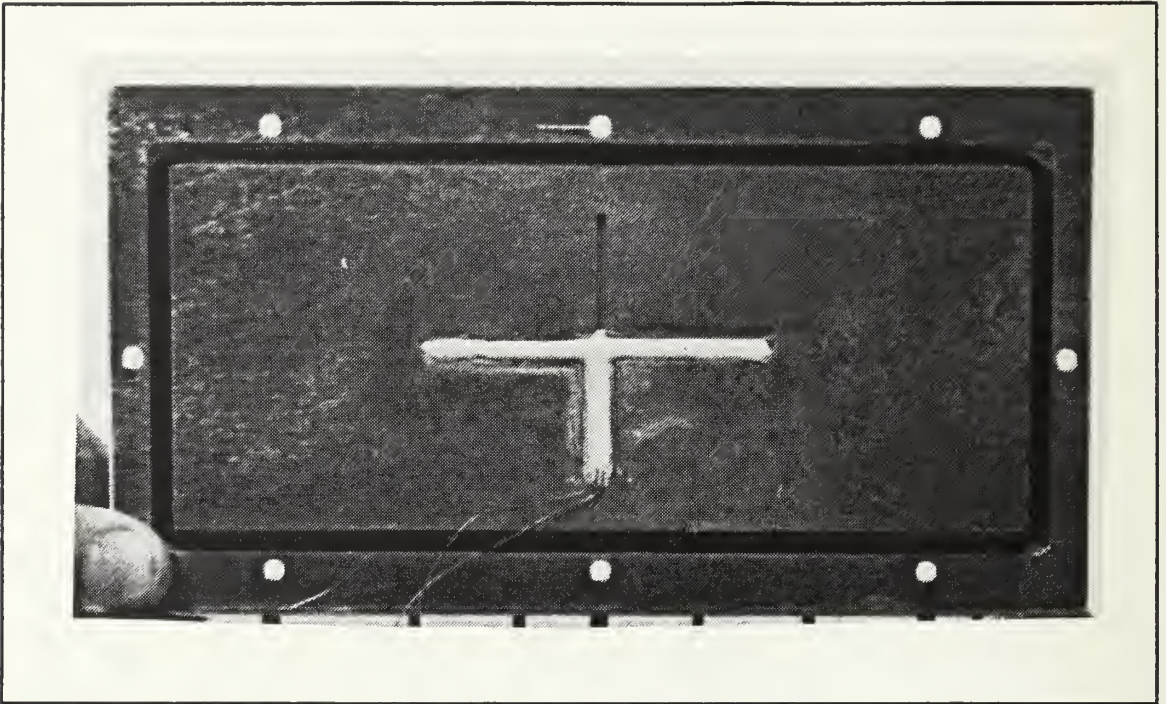


Figure 9. Condensor Surface Details

III. EXPERIMENTAL PROCEDURE

A. PREPARATIONS

Careful preparations were required to ensure that the data obtained was of high quality. The most notable requirement being the necessity of thoroughly degassing the FC-72 liquid, [Ref, 3: p. 3].

1. Normal Warm-Up Procedure

In carrying out the experimental runs the following procedures were followed.

1. Power-up the HP3852A Data Acquisition Unit to start the warm-up period of one hour minimum. [Ref. 13: p. 586]
2. Ensure the liquid level is above Wire 5, but below the condensate drip tray.
3. Set power supply of thermoelectric coolers to 1.3 amps and 2.0 volts.
4. Ensure the experimental chamber's insulation jacket is in place and set power supply to strip heaters to approximately 1.8 amps and 20 volts.
5. Verify the 0.25 inch diameter vent line is unobstructed.
6. Power on the HP300 series desktop computer, and load data acquisition program as contained in Appendix D.
7. Once fluid has reached saturation and is boiling vigorously, hold for a minimum of one hour, typically two hours was achieved, to permit adequate degassing of fluid.

In actual practice, the time required to raise the bulk temperature of the fluid to saturation temperature of 56 °C was nominally two hours.

2. Post Warm-up Procedure

Once the required degassing has been accomplished, power is temporarily secured to the strip heaters. Once power is secured the forward strip heater is electrically isolated. The rear strip heater is powered at 0.9 amps and 20 volts, and the thermoelectric coolers are secured.

The power setting of the strip heaters permits vigorous boiling from its surface. This serves to keep the fluid degassed and the bulk fluid temperature near saturation and near isothermal. By keeping the fluid level below the insert board's upper edge, the fluid forward of the insert board remains undisturbed by the boiling action occurring in the rear chamber.

B. DATA ACQUISITION PROCEDURE

Upon completion of the previous preparatory procedures, the experimental runs are ready to begin. The procedure followed for an experimental run is as follows:

1. Plug power supply into power receptacles for wire 1. Power on and ensure current limiter is set to max value of 1.0 amps.
2. Plug HP6214C power supply into power receptacles of desired constant heat flux wire.
3. Set power supply of step 2 to proper output to give desired heat flux from the wire.
4. Start running the Data Acquisition Program, which is programmed to measure the following data from the desired wires at two minute intervals.
 - Precision Resistor Voltage drop, up to five channels.
 - Platinum Wire Voltage drop, up to five channels.
 - Four bulk fluid temperature measurements
 - Two condenser surface temperature measurements.
 - One ambient air temperature measurement.
5. After each data interval, increase the voltage to the varying heat flux wire by 0.2 Volt increments. This was continued until the on line power supply was at 2.3 volts of outputs, the increments were then reduced to 0.1 volts until nucleation occurred. The increments were then returned to 0.2 volts until a heat flux of approximately 200,000 watts/m² were achieved. At any higher heat flux the wire will go into the film boiling regime.
6. Reduce the power to the varying heat flux wire at 0.3 Volts increment to bring the wire back to a no power condition.
7. Repeat steps 3 thru 6 for all other wire and heat flux configurations.

C. DATA REDUCTION

Data that was obtained from the actual experimental apparatus were two voltage measurements per active platinum wire channel, and six temperature measurements. The process used for data reduction is a combination of computer programs and graphical outputs for numerical presentation and visual presentations respectively.

1. Numerical Data

The numerical data values required to be processed are:

1. Fluid Bulk Temperature

$$T_{bulk} = \frac{(T_1 + T_2 + T_3 + T_4)}{4.0} (^{\circ}\text{C}) \quad (3.1)$$

and where, T_1 thru T_4 are the thermocouple measurements of the bulk fluid.

2. Current flow through the Platinum Wire, where

$$I_{wire} = \frac{V_{Res}}{R_{2\Omega}} \text{ (Amps)} \quad (3.2)$$

3. Platinum Wire's electrical resistance value, where

$$R_{PtWire} = \frac{V_{PtWire}}{I_{wire}} \text{ (Ohms)} \quad (3.3)$$

4. Platinum Wire surface temperature, where

$$T_{sur} = \varepsilon R_{PtWire} + T_o(^{\circ}\text{C}) \quad (3.4)$$

where,

T_{sur} = the actual wires surface temperature

ε is the slope of the calibration curve

T_o is the calibration curves y-axis intercept

5. Fluid Film Temperature, where

$$T_{film} = \frac{T_{sur} + T_{bulk}}{2.0} \quad (3.5)$$

6. Dissipated Heat Flux of platinum wire, where

$$q = \frac{I_{wire} \times V_{PtWire}}{\text{Area}_{Surf}} \left(\frac{\text{Watts}}{\text{m}^2} \right) \quad (3.6)$$

where, $\text{Area}_{Surf} = \pi \times \text{length}_{wire} \times D_{wire}$

The above numerical data were all derived from the raw data, and previously determined calibration curves. The following table provides physical dimensions and temperature calibration coefficients of the platinum wires.

Table 2. PLATINUM WIRE PHYSICAL PARAMETERS FOR EQUATION (3.4) AND EQUATION (3.5)

Wire	ε	T_o	length	diameter
	$^{\circ}\text{C}/\Omega$	$^{\circ}\text{C}$	mm	mm
1	53.902	-254.470	99.22	0.05
2	53.666	-253.009	99.22	0.05
3	53.141	-252.729	100.01	0.05
4	53.484	-252.848	98.43	0.05
5	53.086	-260.049	100.01	0.05

To see in detail the methodology used to obtain the numerical values presented in the preceding table, proceed to Appendix A 'Platinum Wire Calibration'.

2. Fluid Property Data

The Fluid Properties to be determined are as follows:

1. **Thermal Conductivity of fluid**, as obtained from Figure 5 of the 3M Corporation Fluorinert Product Manual [Ref. 3: p. 15] have been determined to be,

$$k = \frac{0.6033 - 0.00115 \times T_{film}}{10.} \left(\frac{\text{Watts}}{^\circ\text{C}} \right) \quad (3.7)$$

2. **Thermal Expansion Coefficient**, from table 4B in the Product Manual [Ref. 3: p. 10] is given as

$$\beta = \frac{0.00261}{1.740 - 0.00251 \times T_{film}} \left(\frac{1}{^\circ\text{C}} \right) \quad (3.8)$$

3. **Kinematic Viscosity of the Fluid**, as obtained from Figure (3) in the Product Manual [Ref 3: p.13] and determining an exponential curve fit yields

$$\nu = 1.203952E-8 \times \exp(1,058.4109^\circ \frac{\text{K}}{T_{bulk} + 273.15^\circ\text{C}}) \left(\frac{\text{m}^2}{\text{s}} \right) \quad (3.9)$$

4. **Specific Heat of the Fluid** for all the Fluorinert Fluids are obtained from Figure (4) of the Product Manual [Ref 3 : p. 14] is,

$$C_p = (0.24111 + 3.70374E - 4 \times T_{bulk}) \times 4186 \left(\frac{\text{J}}{\text{kg}^\circ\text{C}} \right) \quad (3.10)$$

5. **Liquid Density of FC-72**, from expression in table 4B and constants from table 4C in the Product Manual [Ref 3: p 10] is given by

$$\rho = (1.740 - 0.00261 \times T_{bulk}) \times 1000 \left(\frac{\text{kg}}{\text{m}^3} \right) \quad (3.11)$$

6. **Thermal Diffusivity of the liquid** is given by,

$$\alpha = \frac{k}{\rho \times C_p} \quad (3.12)$$

7. **Prandtl Number of the Fluid** is given by

$$\text{Pr} = \frac{\nu}{\alpha} \quad (3.13)$$

8. **Ralyeigh Number of Fluid** based on wire diameter is given by,

$$\text{Ra} = \frac{g \times \beta \times (T_{sur} - T_{bulk}) \times D^3}{\nu \times \alpha} \quad (3.14)$$

9. **Correlation for the Nusselt Number** was obtained by using the correlation of Kuehn and Goldstein [Ref 10: p. 1128] given by

$$\overline{\text{Nu}}_D = \frac{2}{\ln \left[1 + \frac{2}{\left[(0.518 \times \text{Ra}_D^{1/4} \times \left[1 + \left(\frac{0.559}{\text{Pr}} \right)^{3/5} \right]^{-5/12} \right)^{15} + (0.1 \times \text{Ra}_D^{1/3})^{15} \right]^{1/15}} \right]} \quad (3.15)$$

10. **Theoretical Heat Flux** as obtained from using the \bar{N}_D value obtained from equation (3.15).

$$q = \frac{k \times \bar{Nu}_D \times (T_{sur} - T_{bulk})}{D} \left(\frac{\text{Watts}}{\text{m}^2} \right) \quad (3.16)$$

With all the required numerical data and fluid properties obtained, it is now necessary to present the numerical information in a graphical representation to see the relevancy of the results obtained. This will become apparent with the presentation of results in Chapter IV 'Results and Discussion'.

IV. RESULTS AND DISCUSSION

The data obtained can be grouped for discussion as follows:

1. Individually powered wires
 - Saturated Conditions
 - Sub-Cooled Conditions
2. Bubble Pumping Effect Runs
 - Saturated Conditions
 - Sub-Cooled Conditions

A. INDIVIDUALLY POWERED WIRES

Before analyzing the pumping effect of the bubbles on the upper wires, the individual wire boiling experiments will be investigated. All of the individual powered wire runs shown here were made at or near saturated fluid conditions with two exceptions. The following table will provide a listing of single wire runs.

Table 3. INDIVIDUAL WIRE RUNS

Figure	Wire	T_{bulk}
Figure 10	1	55.5° C
Figure 11	1 - several runs overlayed	At or near saturation
Figure 12	1	38° C
Figure 13	1	23.0° C
Figure 14	2	56.0° C
Figure 15	3	56.0° C
Figure 16	4	56.0° C
Figure 17	all the above	see individual wires

In all cases conditions were under atmospheric pressure with 0.05mm diameter platinum wires.

1. Natural Convection

Figure 10 is a typical boiling curve for FC-72 with the Kuehn and Goldstein natural convection region shown along with the experimental points. The nucleate boiling zone starts at boiling incipience, which is evident from the sudden drop of wall temperature, a characteristic of a highly wetting fluid. Figure 11 is a compilation of wire

1 data, at or near saturation, obtained over a period of time. As can be seen, with the exception of the boiling incipience point, the data is virtually super imposable over each other. This reproducibility of data over time indicates no significant aging has occurred on wire 1, and more importantly no change in calibration.

In fact in the natural convection region Figure 10 thru Figure 16 are all essentially superimposable over each other. Figure 17 is an overlay of all the previous figures. Therefore, it appears that whether the fluid is Saturated or Sub-Cooled, the fluid bulk temperature appears to have little effect on the natural convection heat transfer rate.

There was generally very good agreement between the natural convection data and the Kuehn and Goldstein correlation [Ref 10] (equation 3.15). The only deviation existing between the figures being the total temperature excursion to incipience, which ranged from 27° C to 38° C.

2. Nucleate Boiling

As previously stated, the nucleate boiling zone starts at boiling incipience. Using wire 1 as a standard and Figure 10 as base line boiling characteristic data a comparison to other wires at saturation condition, and a comparison to subcooling effects on wire's 1 boiling can be made. As is evident from Figure 17, the boiling characteristic of all the wires at saturation condition tend to overlap each other. The differences arising tending to be caused by individual wire placement in the fluid. However, the effect of subcooling does result in a decrease in the boiling curve overshoot at point of incipience. This decrease in the boiling curve overshoot results in a net decrease in the superheat required to initiate nucleate boiling.

3. Departure from Nucleate Boiling

The Critical Heat Flux (CHF) for FC-72 at saturated condition was calculated by Danielson et al [Ref 9] to be approximately 203,000 Watts/m². Experimental value for CHF ranged from 198,000 Watts/m² to 220,000 Watts/m², a spread of -2.5% to 8.4%. A CHF for a subcooled condition of $T_{bulk} = 38^{\circ} \text{C}$ was found experimentally to be approximately 400,000 watts/m². A CHF for $T_{bulk} = 23^{\circ} \text{C}$ was not obtained during the experimental runs.

WIRE 1 BOILING CURVE

NEAR SATURATION $T_{bulk} = 55.5^\circ \text{Celsius}$

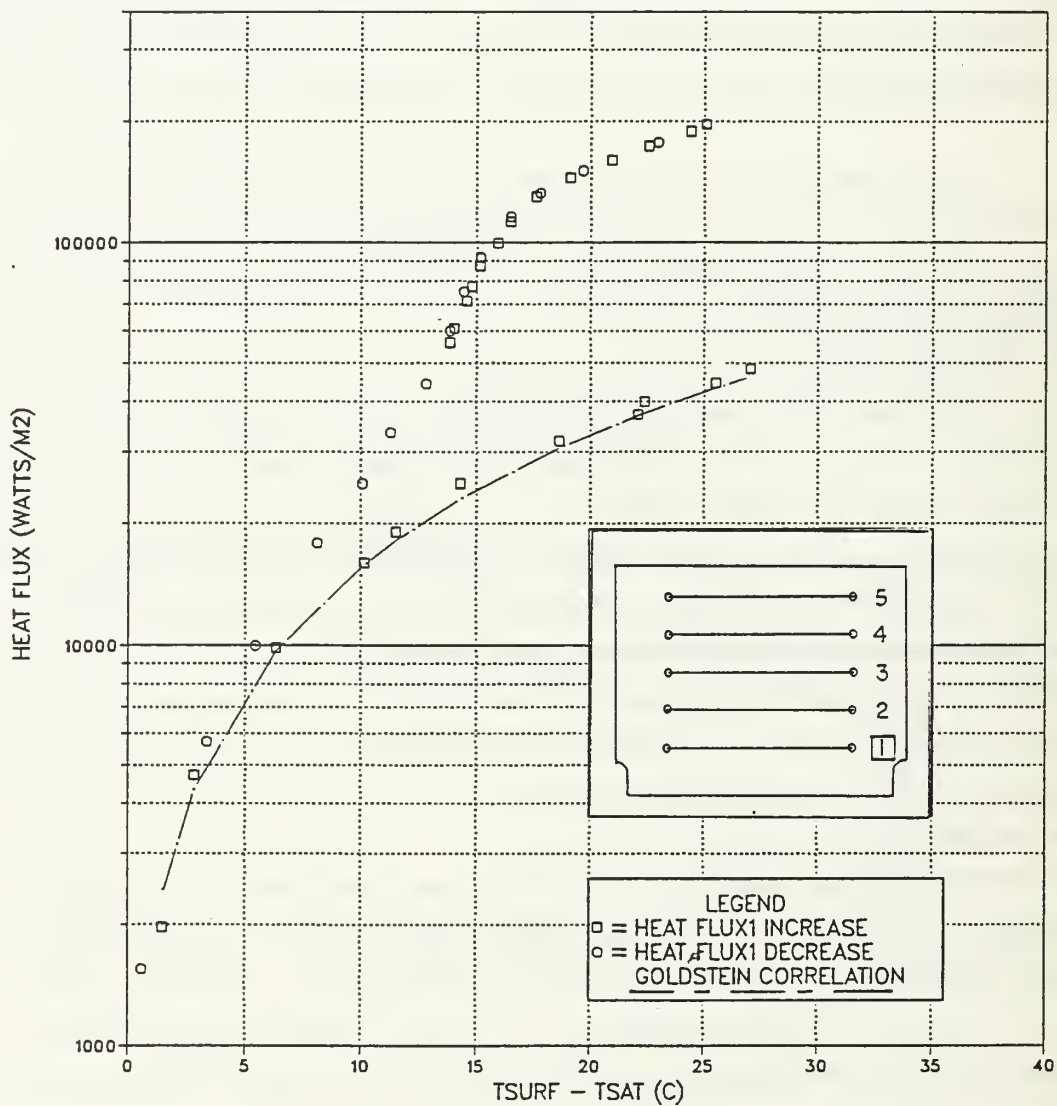


Figure 10. Wire1 boiling curve $T_{bulk} = 55.5^\circ \text{C}$

WIRE 1 BOILING CURVES

ALL BOILING CURVES AT SATURATION OR NEAR SATURATION

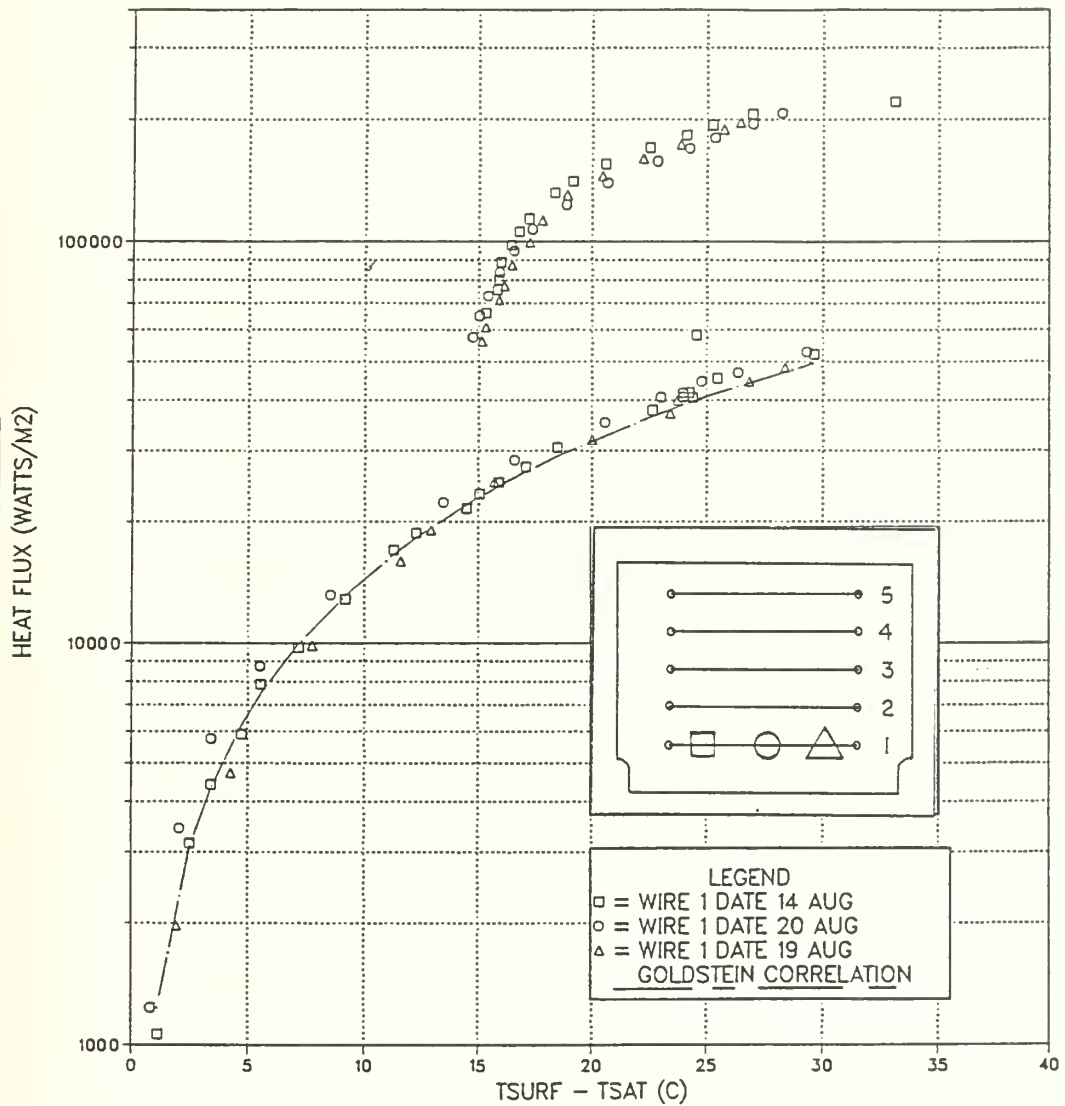


Figure 11. Wire 1 Boiling Curves over time

WIRE 1 BOILING CURVE

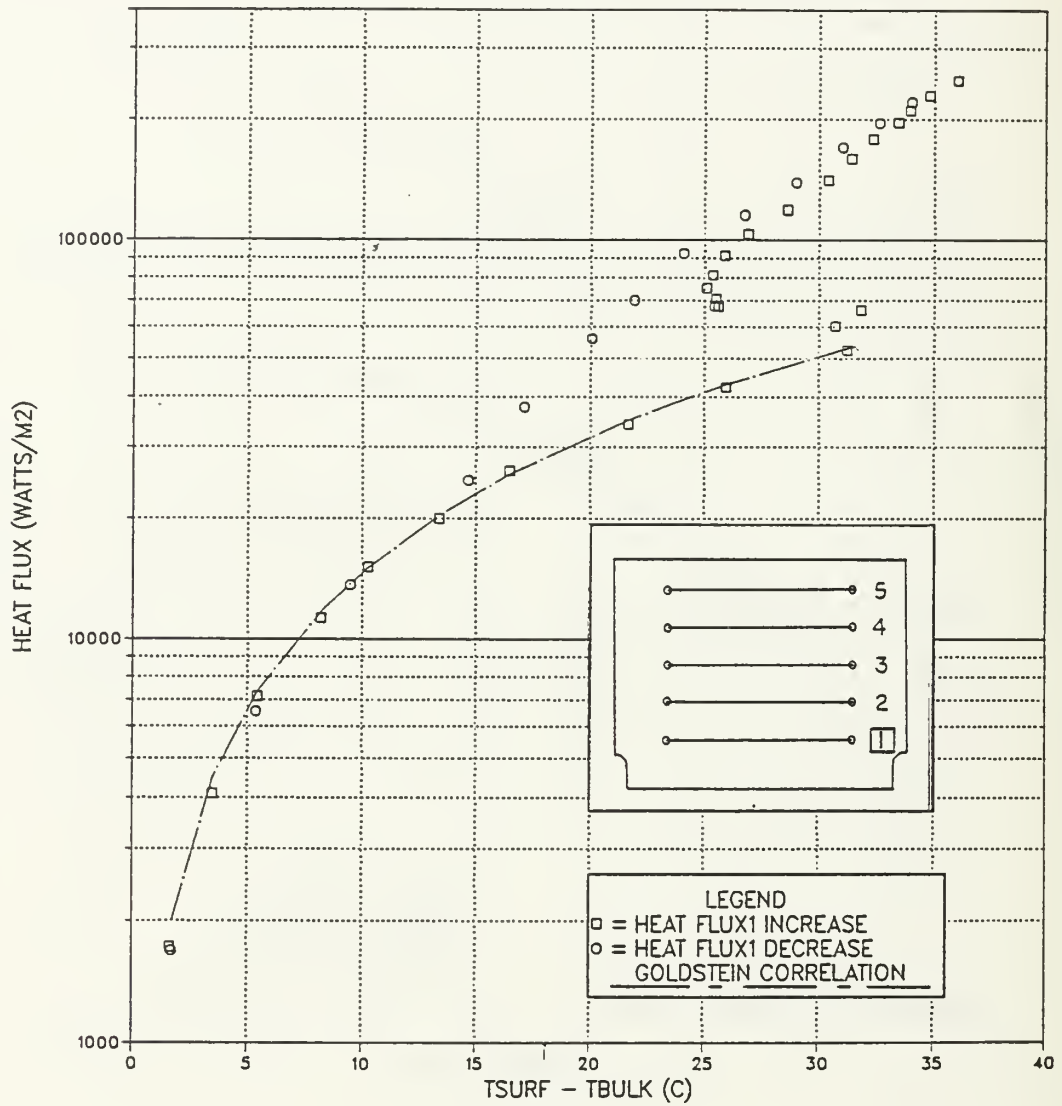


Figure 12. Wire 1 boiling curve $T_{bulk} = 38^{\circ}\text{C}$

WIRE 1 BOILING CURVE

.SUBCOOLED $T_{bulk} = 22.5^\circ \text{Celsius}$

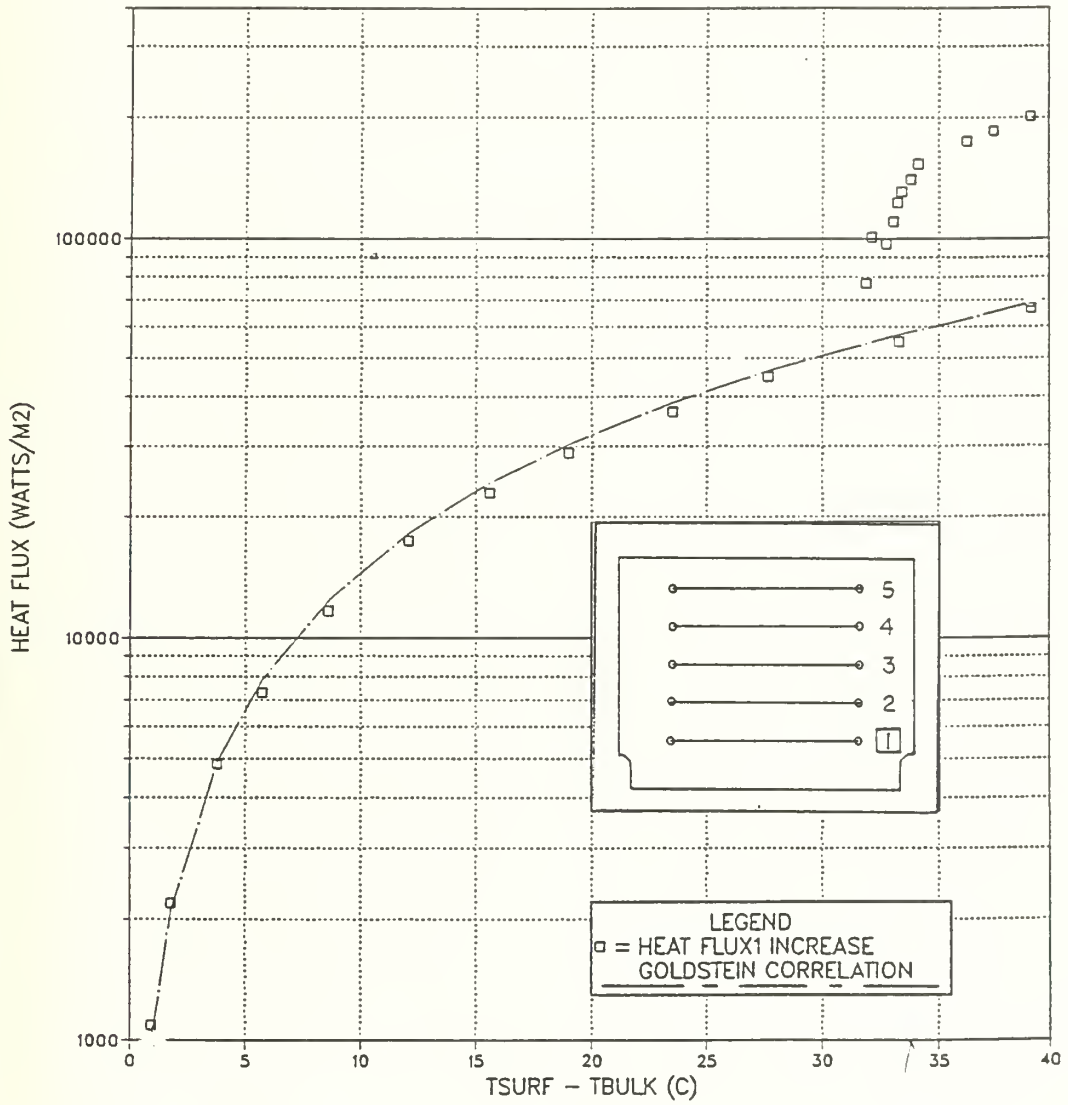


Figure 13. Wire 1 Boiling Curve $T_{bulk} = 23^\circ \text{C}$

WIRE 2 BOILING CURVE

SATURATED $T_{bulk} = 56.0^\circ \text{Celsius}$

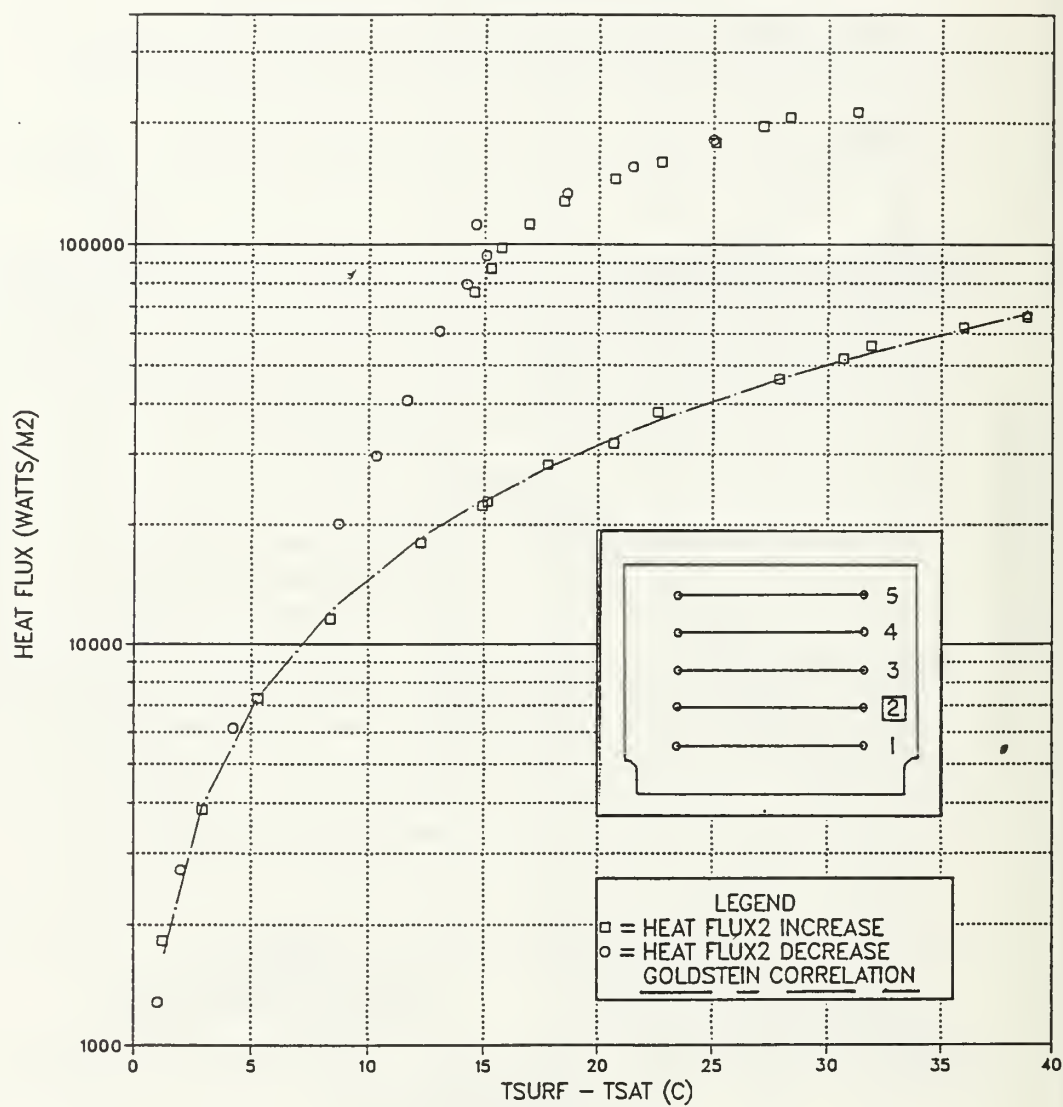


Figure 14. Wire 2 boiling curve $T_{bulk} = 56^\circ \text{C}$

WIRE 3 BOILING CURVE

SATURATED $T_{bulk} = 56.0^{\circ}\text{Celsius}$

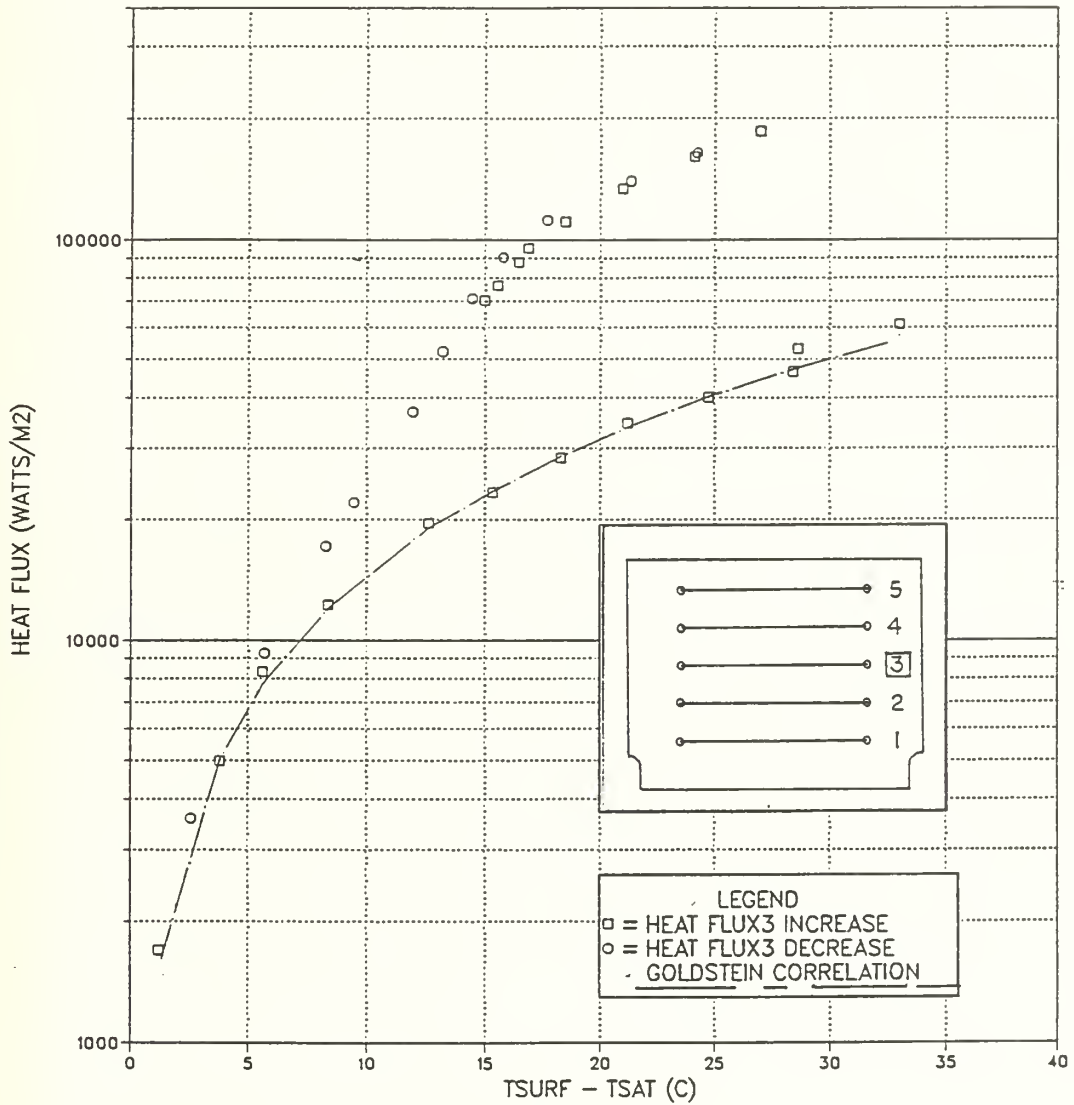


Figure 15. Wire 3 Boiling Curve $T_{bulk} = 56^{\circ}\text{C}$

WIRE 4 BOILING CURVE

SATURATED $T_{bulk} = 56.0^{\circ}\text{Celsius}$

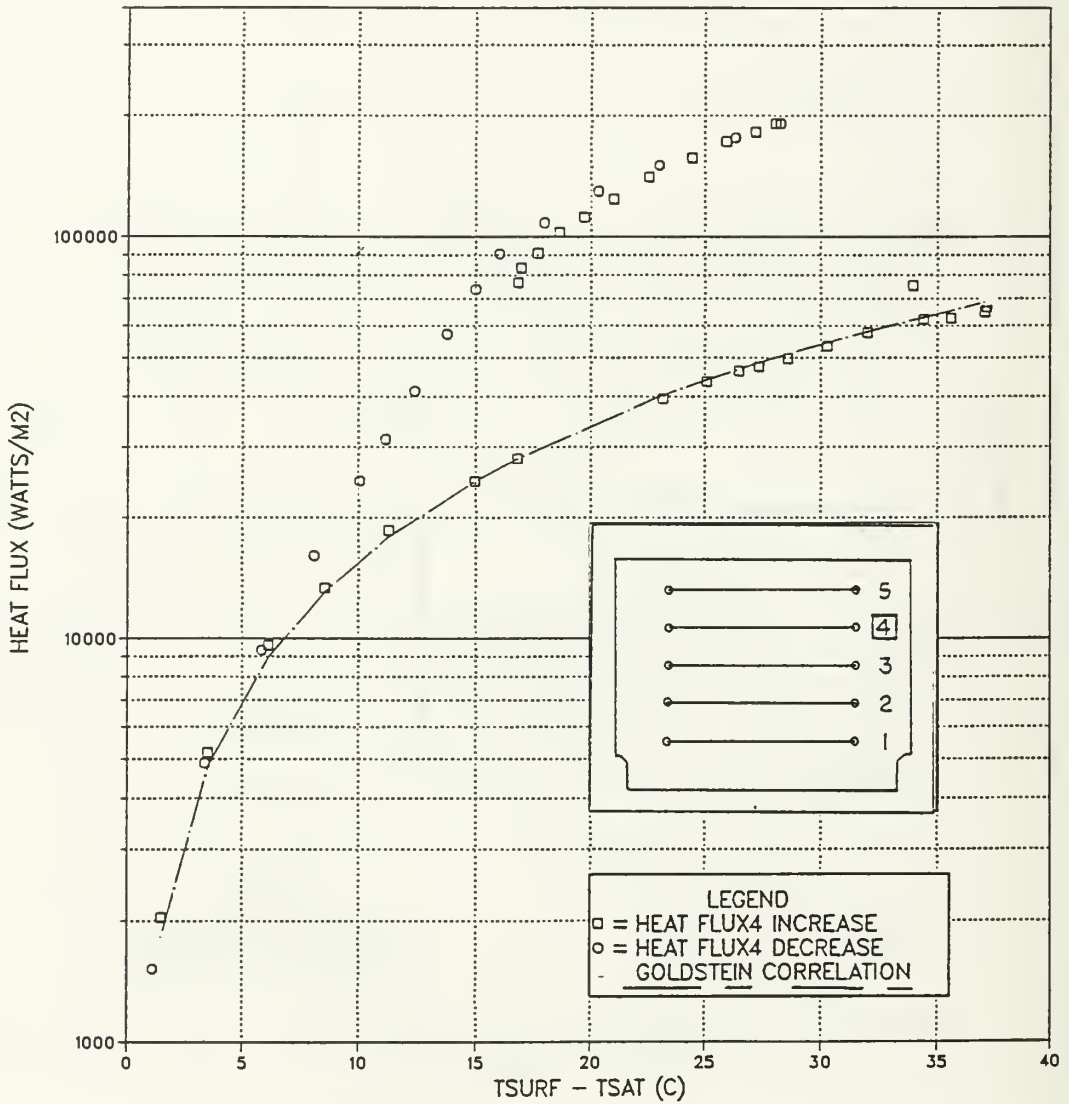


Figure 16. Wire 4 boiling curve $T_{bulk} = 56^{\circ}\text{C}$

BOILING CURVES COMPILED

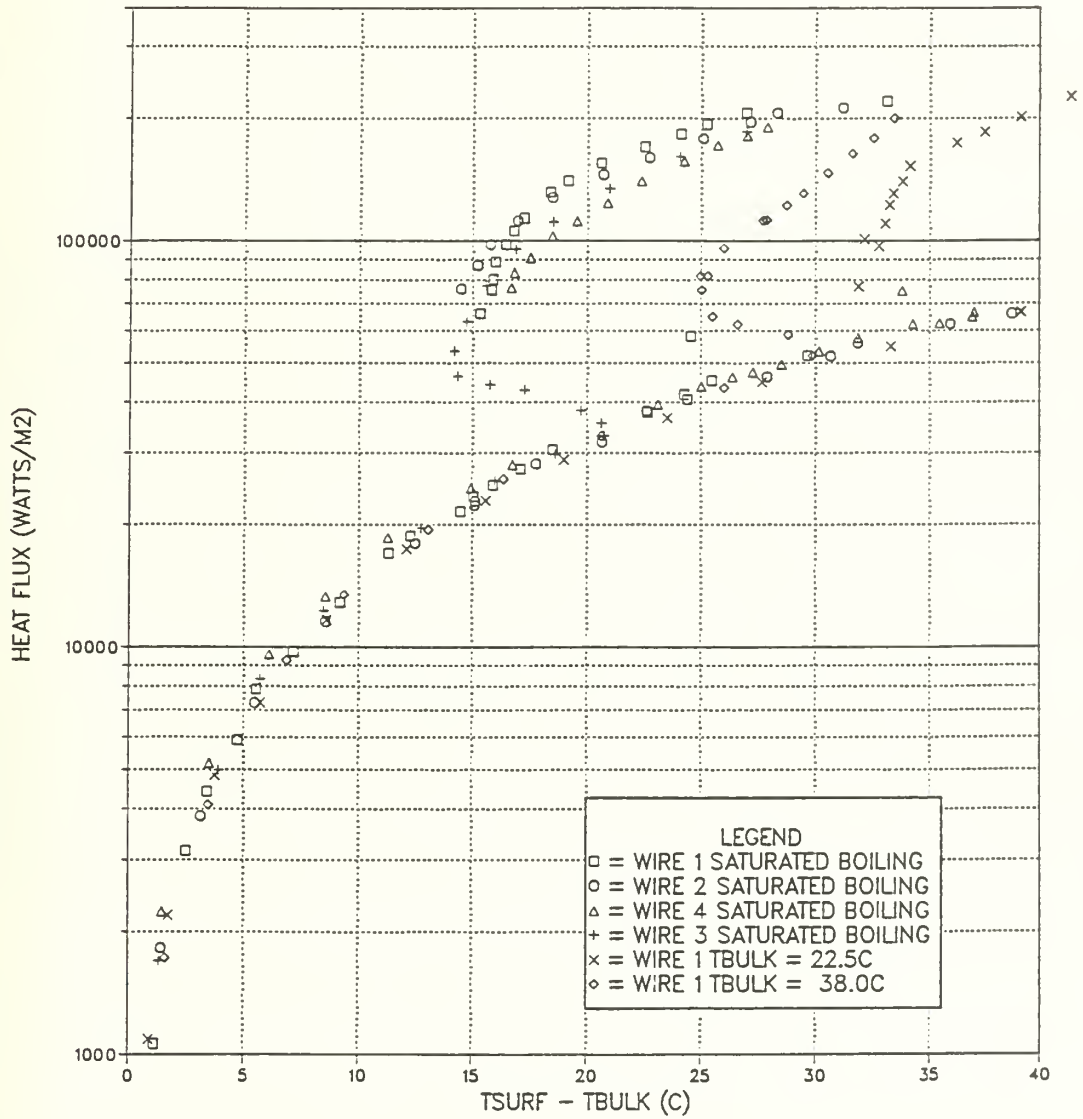


Figure 17. Overlay of previous curves

B. BUBBLE PUMPING EFFECT ON HEAT TRANSFER RATE

In the upcoming discussion a brief explanation of the figures are required. In each case for these experiments, heater wire number 1 was used to generate the bubbles for examining the pumping effects upon the upper wires. The figure insert is used to show which wires are being utilized. Only select data points were plotted for the passive (constant heat flux wire) wire, and those points correspond in time to the identically numbered data point on wire 1's boiling curve. The data points were chosen since they define regions of wire 1's boiling curve as shown in the following table.

Table 4. DATA POINT DESCRIPTION

5 point figure	6 point figure	Region Description
1	1	Natural Convection Start
2	2	Point of Incipience
	3	Partial Boiling on wire
3	4	Full nucleate Boiling
4	5	Max Nucleate Boiling
5	6	End of run

1. Passive Wire at Low Heat Flux

In these experimental runs the heat flux on the passive wire was set to approximately 8500 watts/m². At this low heat flux it was expected that little to no active nucleation will occur on the passive wire, even after wire 1 is in nucleate boiling. Therefore, all the enhancement of the upper wire will be due to an addition of a force convection term to the heat transfer rate.

In comparing Figure 18 to Figure 19 the following can be inferred:

1. Total reduction of wall temperature on the passive wires are comparable. Wire 2 having a 3.7°C and Wire 4 having a 3.0° C drop in wall temperature.
2. A definite effective distance exist over which wire's 1 influence is imparted upon the upper wires, for example:

Wire 2 and wire 4 showed a very small change in wall temperature at point 2 (point of incipience).

After incipient boiling has occurred on wire 1, wire 2 showed a greater drop in wall surface temperature then wire 4. Approx. 2.5° C drop for wire 2 and 0.1° C drop for wire 4.

3. At point 4, the point of maximum temperature in nucleate boiling, both wire 2 and wire 4 showed a comparable surface temperature, approximately 2°C above saturation.

As can be seen from the figures, some nucleation sites have been activated on wire 2 and wire 4, with point 5 showing a lower wall temperature than point 1.

2. Passive Wire at Medium Heat Flux

In these experimental runs the heat flux on the passive wire was set to approximately $20,500\text{ watts/m}^2$. At this heat flux it was expected that active nucleation will occur on the passive wire after wire 1 is nucleate in boiling.

In comparing Figure 20 to Figure 21 the following can be inferred:

1. The total reduction of wall temperature on the passive wire, points 1 to points 4, are comparable at 7.1°C for wire 2, and 6.3°C for wire 4.
2. The spatial effect is evident on the influence of wire 1 on the upper wires, for example:

Between point 1 and point 2, wire 2 shows a greater reduction in wall surface temperature than is evident in wire 4.

At point 3, wire 2 shows a much greater drop in surface temperature than wire 4: 4°C compared to 2°C . The difference being the amount of

3. At point 4, maximum nucleate boiling from wire 1, both wire 2 and wire 4 show comparable values for surface temperature, approximately 1.3°C .

As can be seen from the figures, wire 1 has activated previously inactive nucleation sites on wire 2 and wire 4. This is evident from point 5 being at a lower surface temperature than point 3.

3. Passive Wire at High Heat Flux

In these experimental runs the heat flux on the passive wire was set to $40,000\text{ Watts/m}^2$ on wire 2 and $35,000\text{ Watts/m}^2$ on Wire 4. At this heat flux it was expected that a large number of inactive nucleation sites will be activated after wire 1 is nucleate in boiling.

In comparing Figure 22 and Figure 23 it is evident that the information obtainable from the figures is comparable to the information for the medium heat flux case. However, the wall temperature reductions on the passive wires are much greater as compared to the Medium Heat Flux case, in particular the following:

1. In comparing the surface temperature reduction from point 1 to point 2, wire 2 has dropped 2.5°C while wire 4 had almost a zero drop of temperature. This appears

to be due to the relative locations of the passive wires with respect to wire 1, and is especially apparent at the higher heat fluxes.

2. Many inactive nucleation sites have been activated by wire 1's nucleation bubbles. As can be seen by comparing point 1 to point 5(6), a difference on Wire 2 of 13° C and on Wire 4 of 7° C is apparent.

4. Wire 1 Passive with Wire 2 varying

In these experimental runs, wire 1 was set to 150,000 Watts/m² so it was boiling vigorously. wire 2 was actively varied over a large heat flux range as can be seen from Figure 24. On Figure 24 a previously obtained boiling curve of Wire 2 was overlayed onto it. Upon comparing the two curves the most striking feature is the disappearance of the Hysteresis Loop as is evident in the overlayed boiling curve data. In this arrangement, the boiling curve overshoot has been removed as a design problem. bubbles from Wire 1 has removed a major design consideration.

5. Subcooled

In these experiments, the bulk fluid was degassed and then subcooled to a temperature of 38° C. In these experimental runs, wire 2 was set at 35,000 watts/m² and 53,000 watts/m², as shown in Figure 25 and Figure 26 respectively. In subcooling, no significant effects were notable beyond those seen in the saturated runs. The only effect that was apparent was the ability to run wire 2 at a greater heat flux with out incipient boiling occuring on the wire.

WIRE 2 AT 8,500 WATT/M2

NEAR SATURATED $T_{bulk} = 55.5^\circ \text{Celsius}$

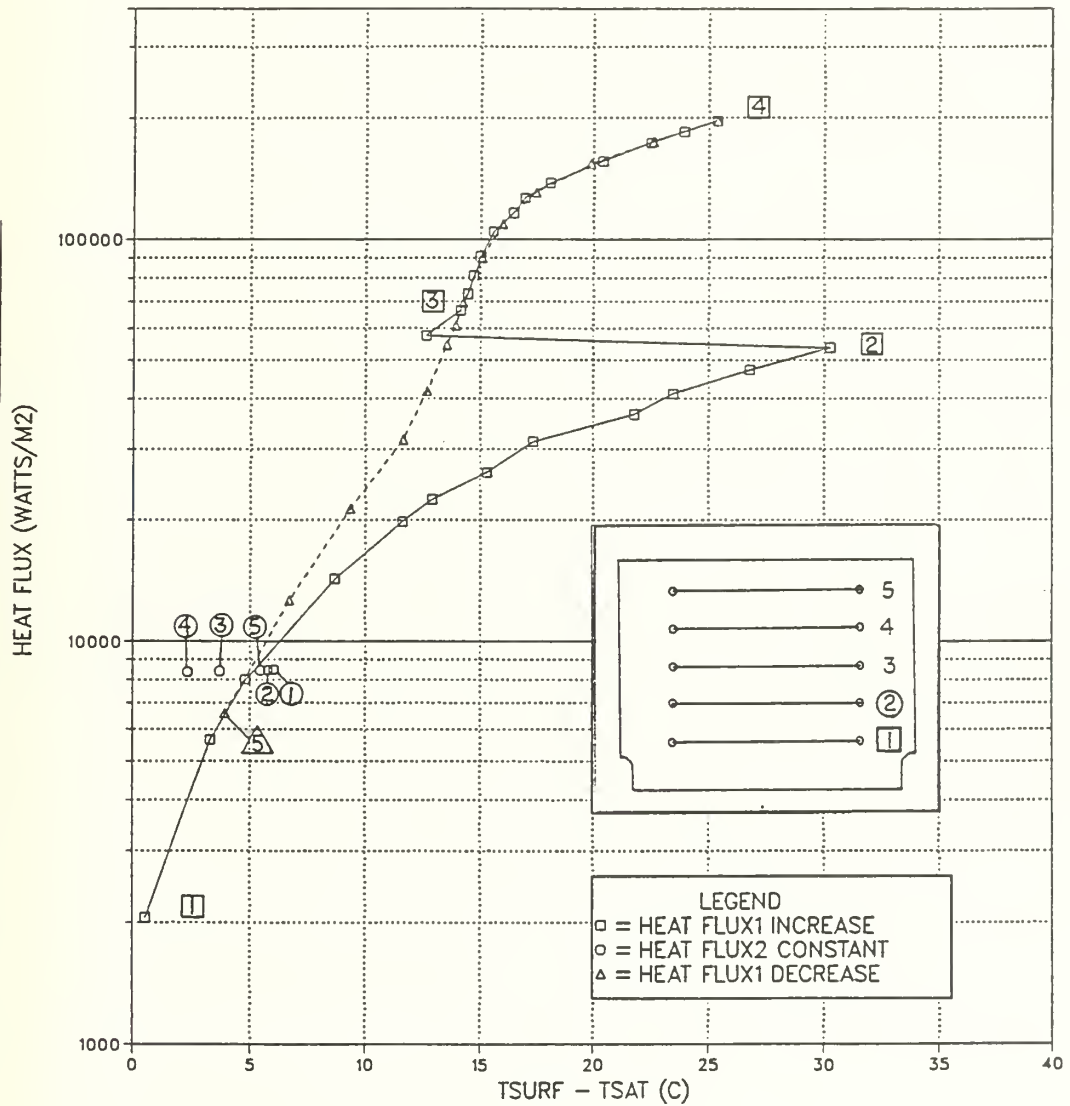


Figure 18. Wire2 at 8500 W/ m² $T_{bulk} = 55.5^\circ \text{C}$

WIRE 4 AT 8,500 WATT/M2

NEAR SATURATION $T_{bulk} = 55.6^\circ \text{Celsius}$

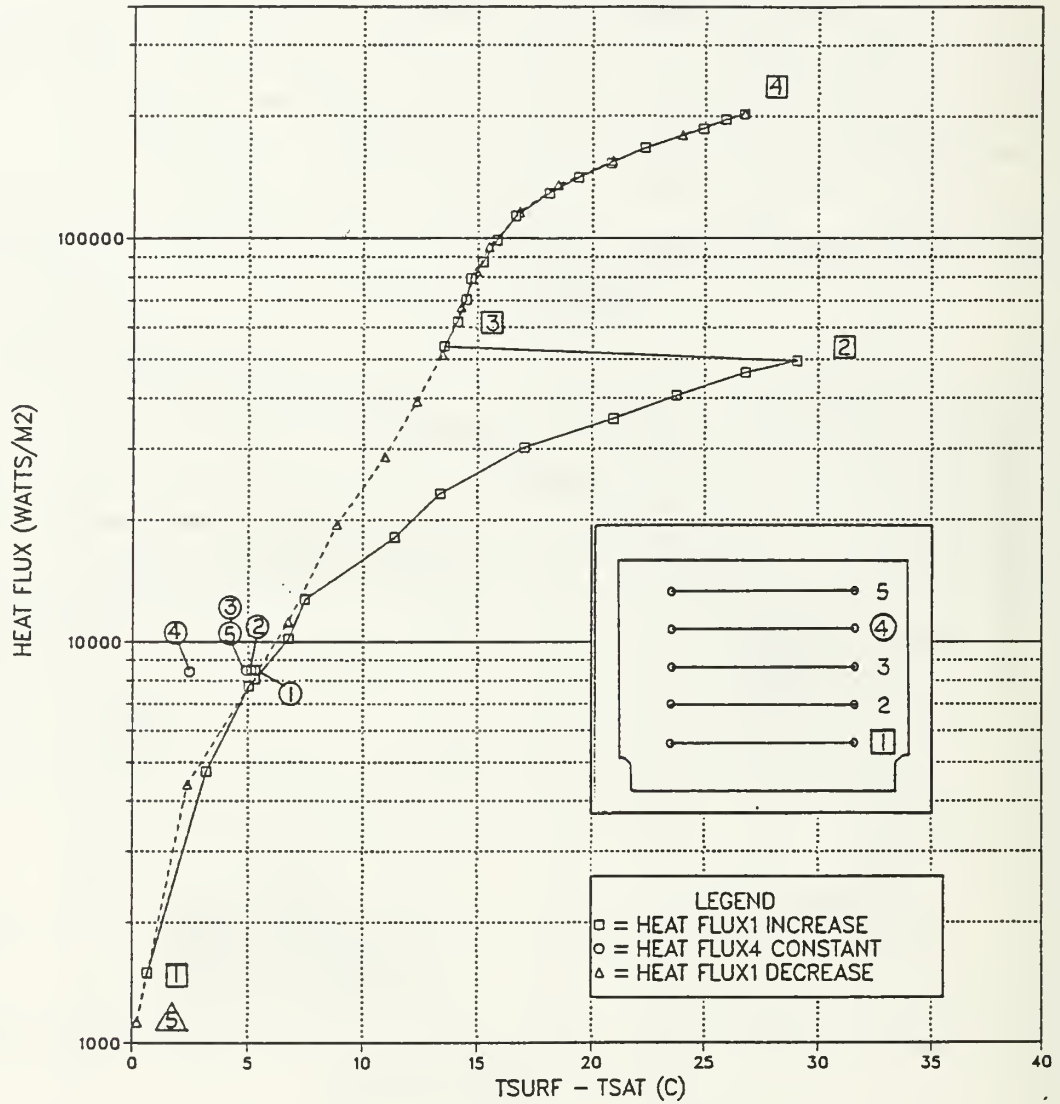


Figure 19. Wire4 at 8500 W/ m² $T_{bulk} = 55.6^\circ \text{C}$

WIRE 2 AT 20,500 WATT/M2

NEAR SATURATION $T_{bulk} = 55.6^{\circ}\text{Celsius}$

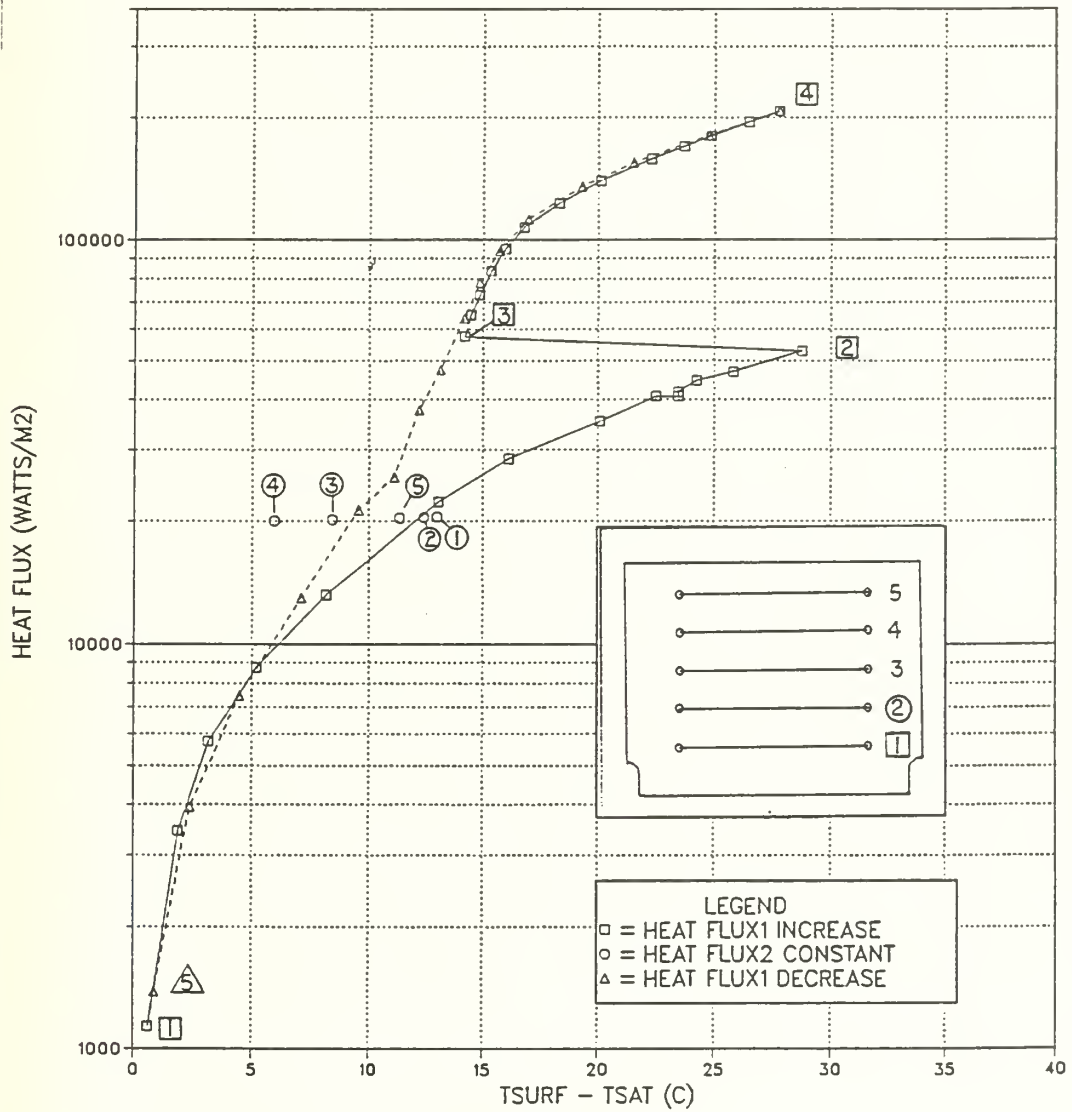


Figure 20. Wire 2 at 20,500 W/ m² $T_{bulk} = 55.9^{\circ}\text{C}$

WIRE 4 AT 20,500 WATT/M2

NEAR SATURATION $T_{bulk} = 55.9^{\circ}\text{Celsius}$

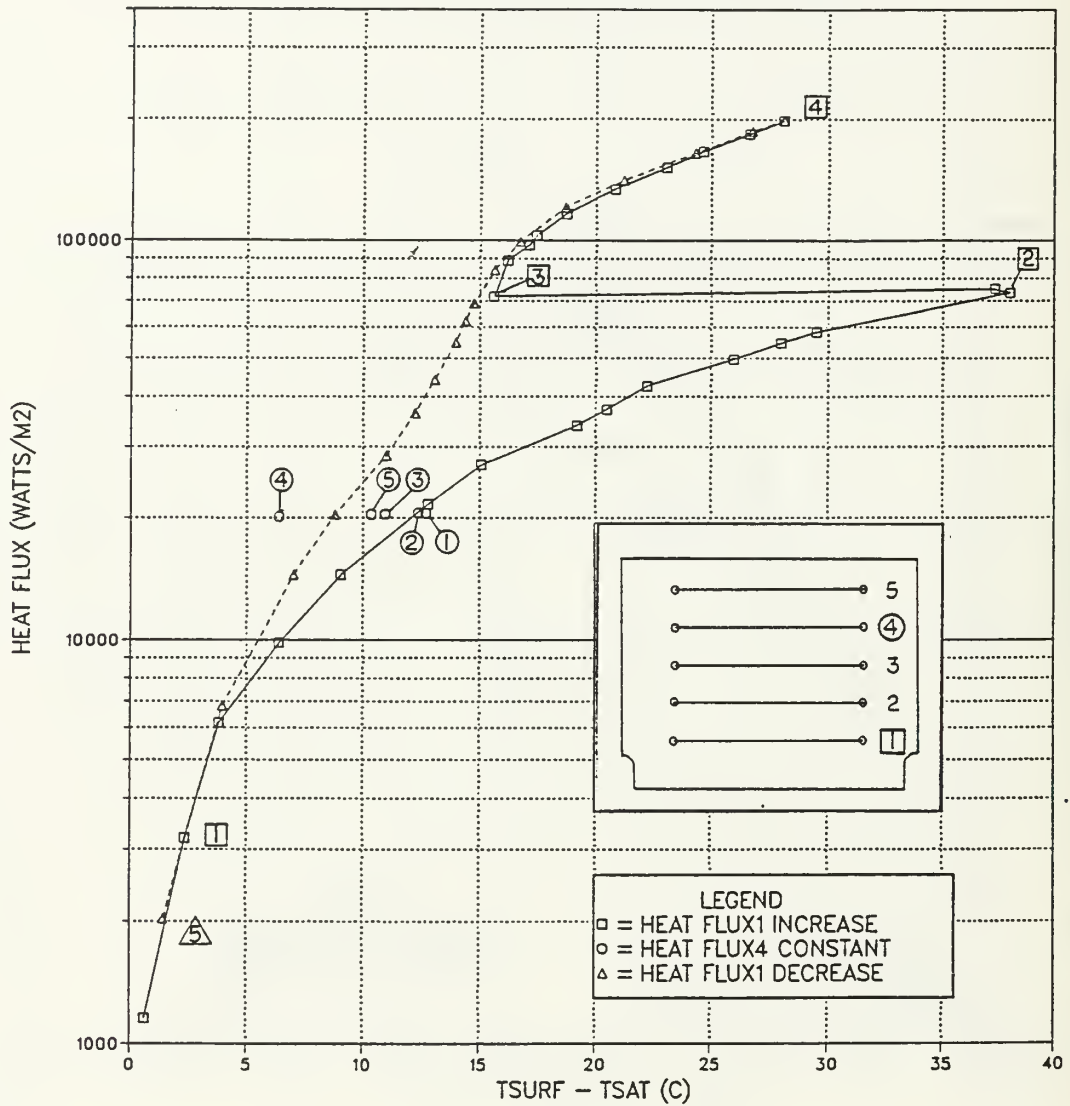


Figure 21. Wire 4 at 20,500 W/ m² $T_{bulk} = 55.6^{\circ}\text{C}$

WIRE 2 AT 40,000 WATT/M2

NEAR SATURATION $T_{bulk} = 54.6^\circ \text{Celsius}$

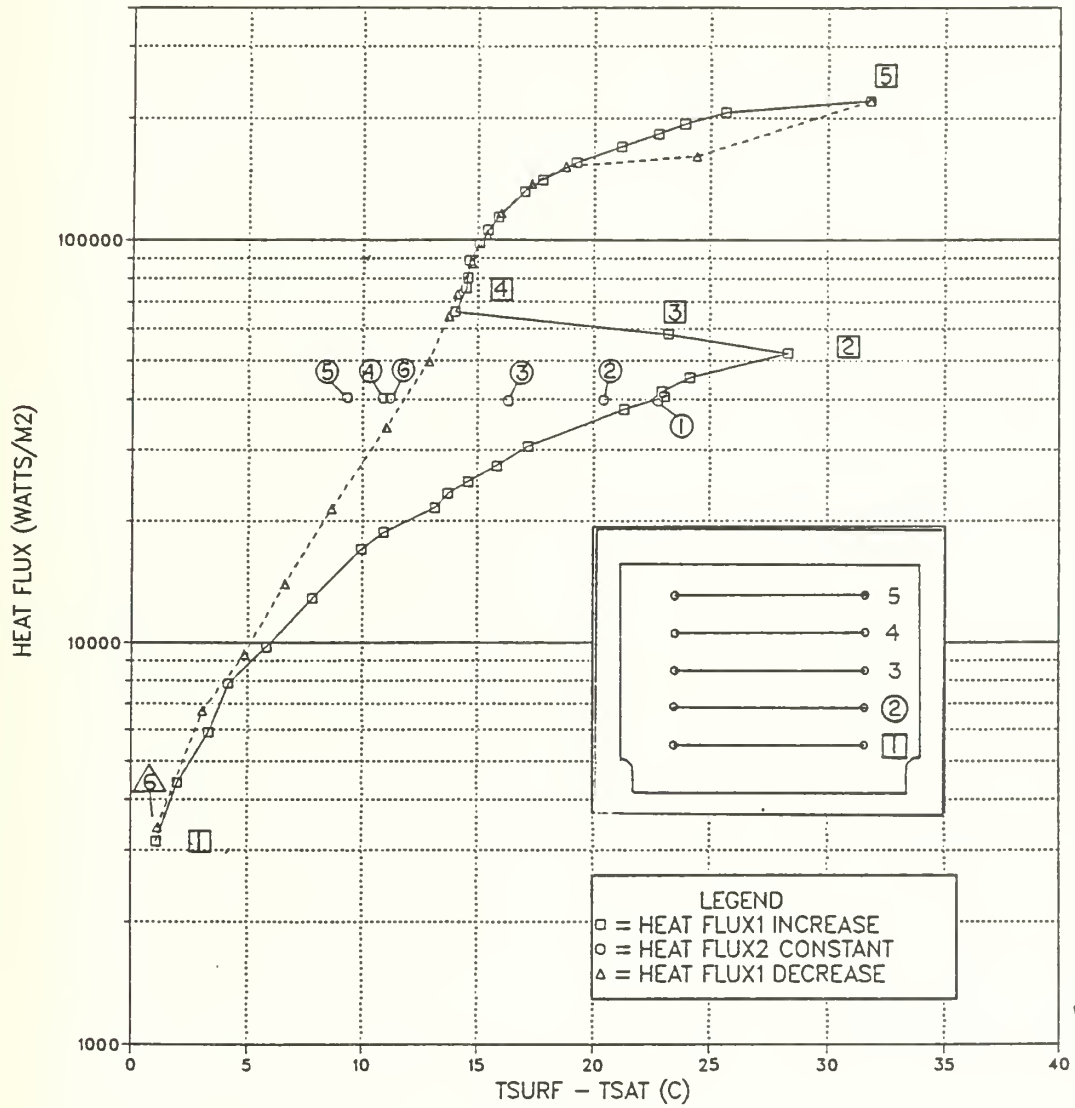


Figure 22. Wire 2 at 40,000 W/ m² $T_{bulk} = 54.6^\circ \text{C}$

WIRE 4 AT 35,000 WATT/M2

NEAR SATURATION $T_{bulk} = 55.0^{\circ}\text{Celsius}$

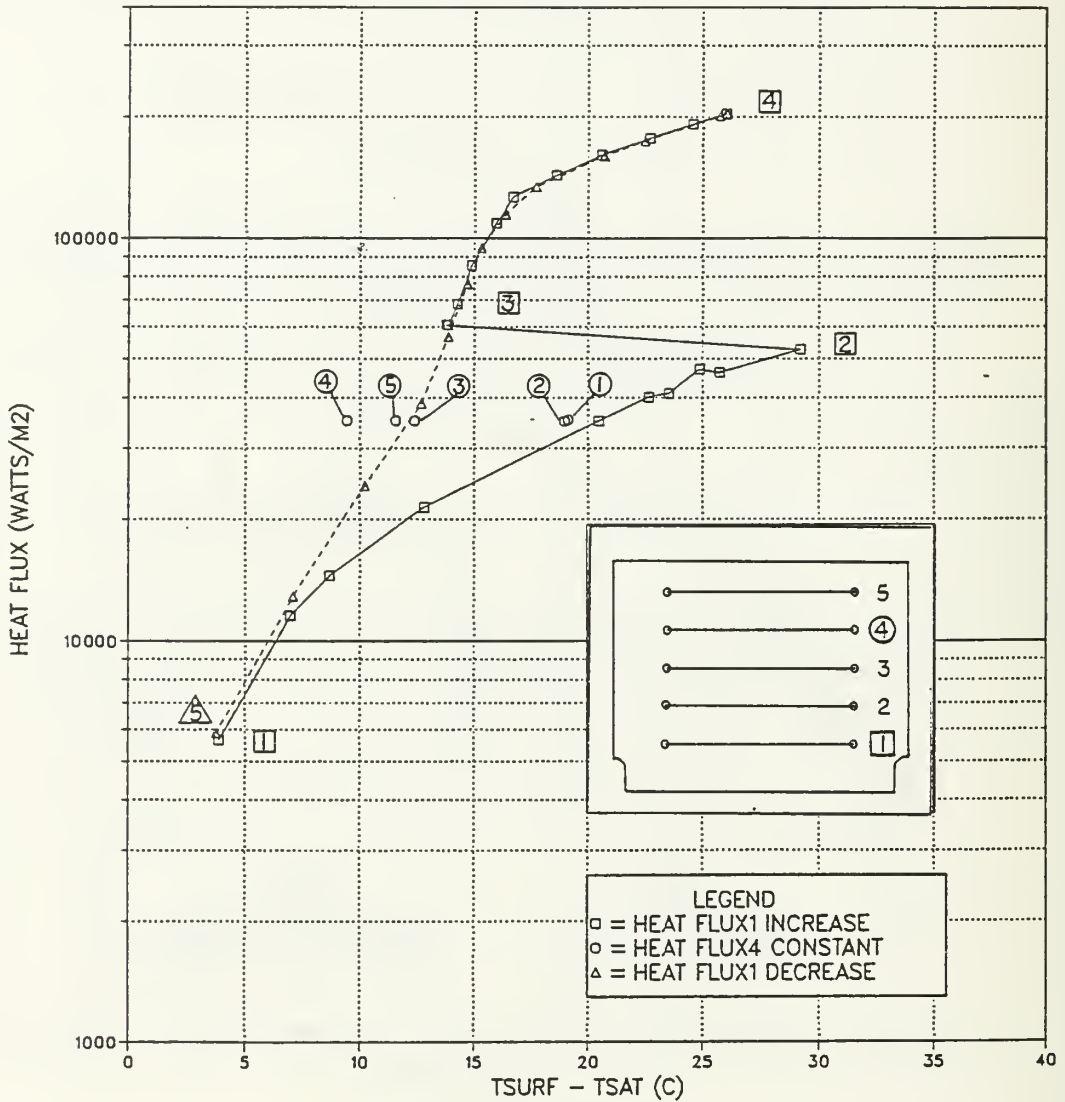


Figure 23. Wire 4 at 35,000 W/ m² $T_{bulk} = 55^{\circ}\text{C}$

WIRE 1 @ 150,000 WATTS/M²

SATURATED $T_{bulk} = 56^{\circ}\text{C}$

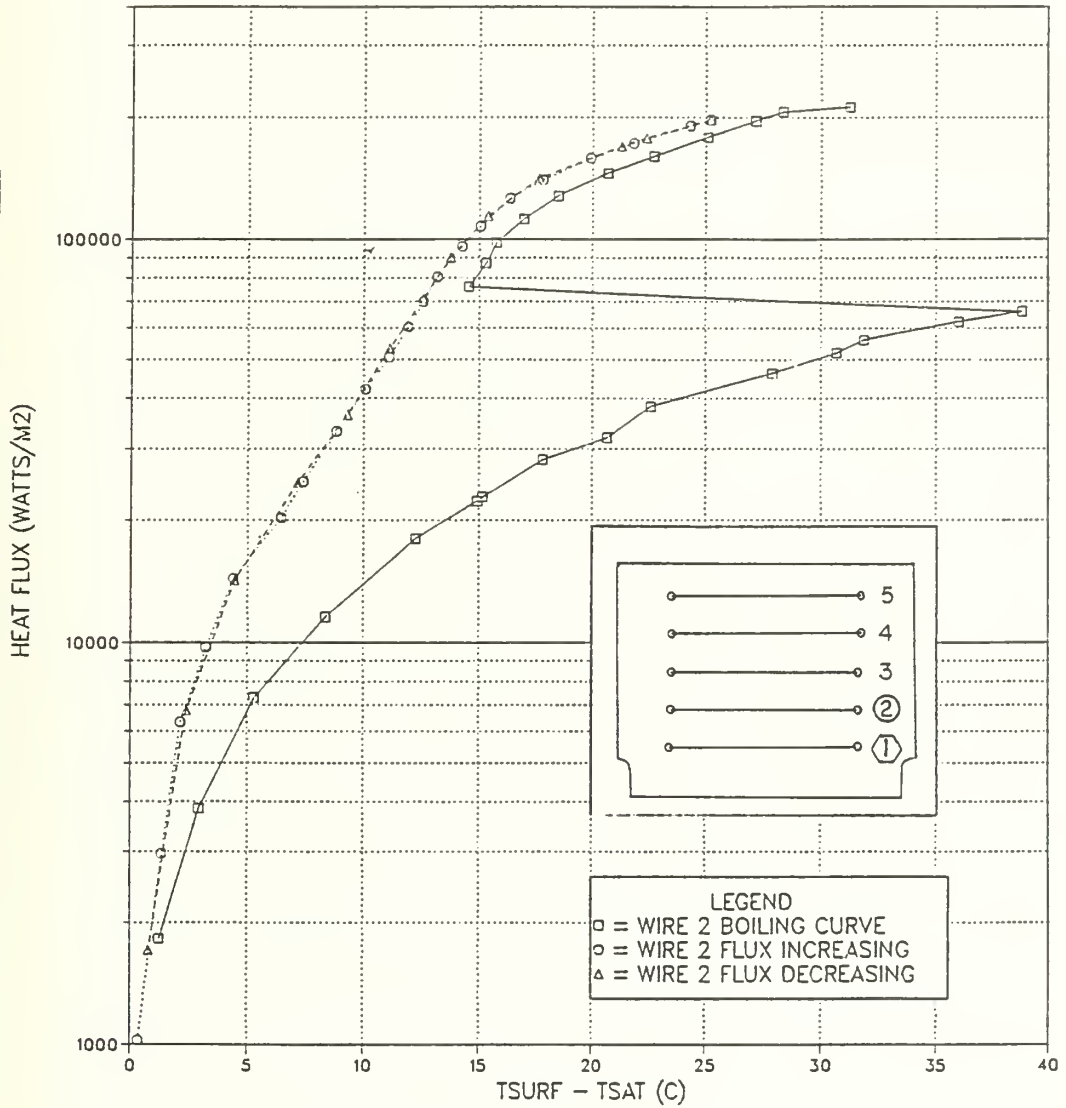


Figure 24. Wire 1 passive, Wire 2 active $T_{bulk} = 56^{\circ}\text{C}$

WIRE 2 AT 35,000 WATT/M2

SUBCOOLED $T_{bulk} = 38.0^\circ \text{Celsius}$

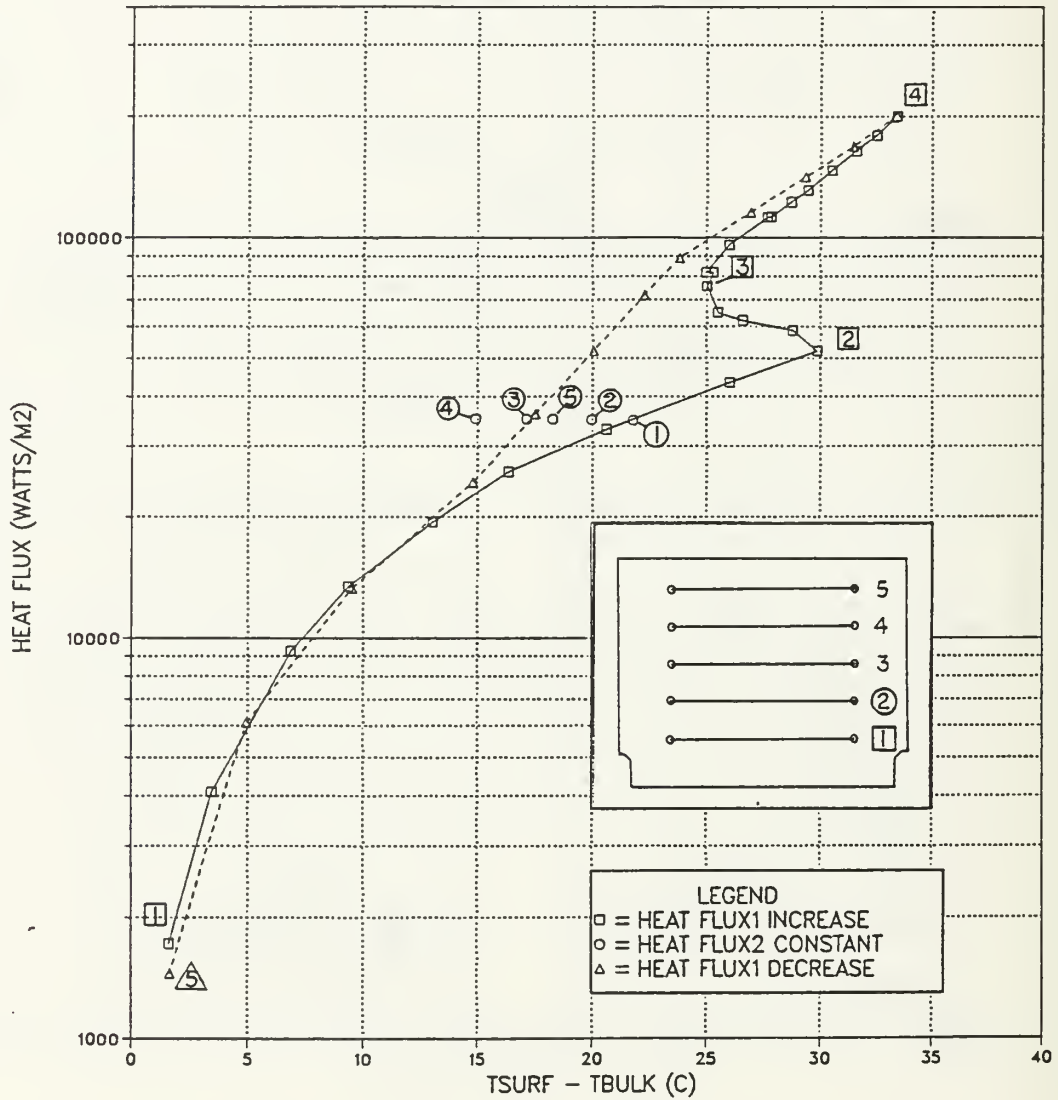


Figure 25. Wire 2 at 35,000 W/ m² $T_{bulk} = 38^\circ \text{C}$

WIRE 2 AT 53,000 WATT/M2

SUBCOOLED $T_{bulk} = 38^{\circ}\text{Celsius}$

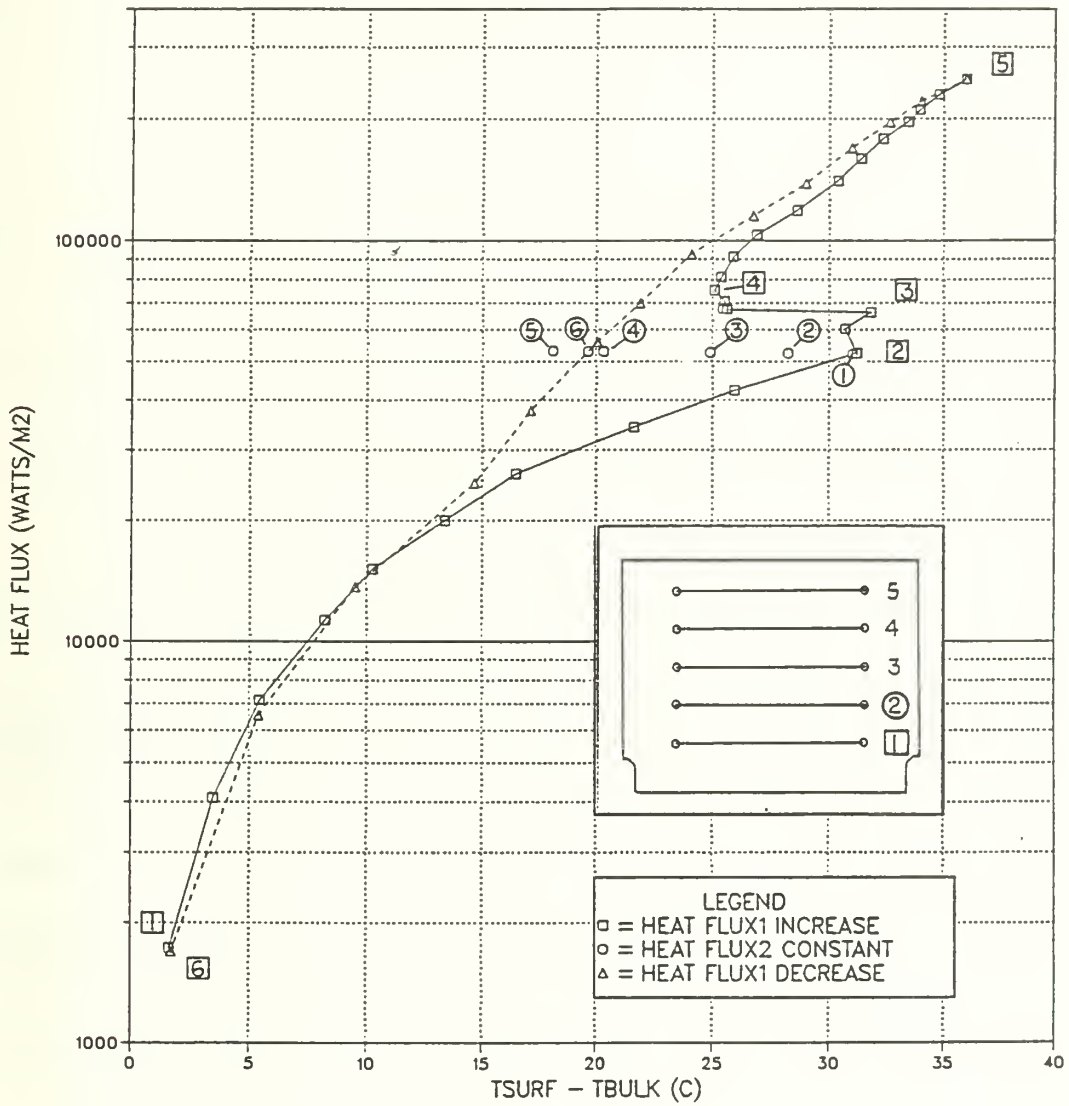


Figure 26. Wire 2 at 53,000 W/ m² $T_{bulk} = 38^{\circ}\text{C}$

V. CONCLUSIONS

The study conducted in this thesis was to investigate the effects of the wake from a bubble generating wire on wires located downstream within the wake. Experimental runs were conducted at saturated condition and subcooled conditions in which the following were found:

A. SINGLE WIRE BOILING

1. The effects of subcooling on the natural convective heat transfer from the wire was negligible.
2. The effects of subcooling tended to increase the heat flux required for incipient boiling to initiate.
3. With subcooling, boiling hysteresis is still observed, but the hysteresis magnitude decreases as subcooling increases.
4. Subcooling results in a reduction in wall temperature after the start of nucleate boiling as compared to saturated cases.

B. PASSIVE WIRE ANALYSIS

Heat Transfer enhancement effects from Wire 1 upon the downstream wires has many factors within it. The following factors have been identified:

1. An enhancement to convection resulting from buoyancy induced fluid flow off of wire 1 was seen to exist. This effect is very spatially dependent with the effects most pronounced on wire 2 and negligible on wire 4. This corresponds to point 1 and point 2 on the figures.
2. The sudden drop of wall temperature between point 2 and point 3/4 was seen to be the results of the following:

Nucleation bubbles from wire 1 activating the inactive nucleation sites on the upper wires resulting in boiling heat transfer off of the upper wires.

An additional force convection enhancement due to the nucleation bubbles from wire 1 breaking up the thermal boundary layer about the upper wires is believed to exist.

3. The drop in temperature on the upper wires corresponding with points 3/4 to point 4/5 appears to be due purely to an increase in force convection due to the high density of bubbles off of wire 1.

Additional conclusions reached are.

1. A constant source of bubble generation from below is an effective way to eliminate the Boiling Curve Overshoot and Hysteresis loop associated with dielectric fluids.

2. At low heat fluxes, proximity to Wire 1 is important for heat transfer enhancement to occur. This dependency reduces as heat flux increase on the passive wire.

APPENDIX A. CALIBRATION

A. PLATINUM WIRE

1. Surface Micro-Structure

Prior to the experiments, a length of 0.05mm platinum wire was analyzed using a Scanning Electron Microscope (SEM). The length of wire analyzed was not used in any experiments, but it did come from the same spool of wire as the experimental lengths of wire, therefore, it should be a representative sample. In analyzing this sample the SEM brought out several important features:

1. From Figure 27 a wire diameter of 0.052mm can be determined. Also, the surface is relatively unmarked at this magnification of 1490x; little scoring on the wire and a low density of surface pits are evident.
2. In Figure 28, an increase in magnification to 4740x within the field of Figure 27, a more detailed view of the larger surface defects are evident. Maximum defect size is approx $2\mu\text{m}$ in length and $0.5\mu\text{m}$ in width. A surface defect of that size would be too large to be a possible nucleation site, according to the calculations done in Ref. 4 of $0.1\mu\text{m}$.
3. In Figure 29, a further increase in magnification to 13,200x within the field of Figure 27, pits of approximately $0.8\mu\text{m}$ max down to $0.3\mu\text{m}$ are seen. It will be these surface defects that boiling will initiate from. The density of these pits along the length of the wire analyzed was not great, this implies that the incipient superheat will be large.

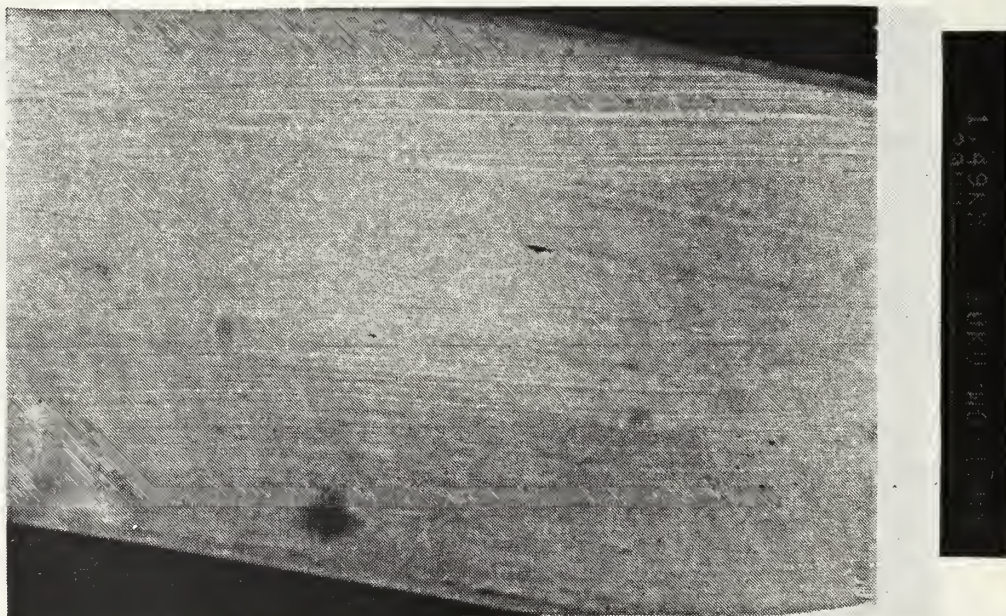


Figure 27. Surface micro geometry: Sample Platinum Wire (1490x)



Figure 28. Surface micro geometry: Sample Platinum Wire (4740x)



Figure 29. Surface micro geometry: Sample Platinum Wire (13,200x)

2. Desirability for Using Platinum

Platinum was chosen for several reasons:

1. It has a highly linear response of Temperature vs Resistance.
2. It has a large ΔR for a given ΔT .

In each aspect, platinum performed very well. As can be seen in the calibration curves of Figure 31 thru Figure 40 response is linear, with a 0.1Ω change in resistance for every 5°C change in temperature.

B. BACKGROUND

An important step in minimizing experimental data uncertainty is an accurate calibration of the platinum wires used. In obtaining the calibration curves for the wires, three calibration runs were performed.

1. An initial calibration in a heated calibration bath with a platinum resistance thermometer.
2. An in place calibration of wires in the test chamber, with the four installed thermocouples used for temperature measurements, was conducted to ensure the calibration curves from the calibration bath were not altered from handling the wire insert board.
3. A final in place calibration of wires in the test chamber, with the four installed thermocouples used for temperature measurements, was conducted to ensure the calibration curves used for data acquisition were not altered due to any reason.

The second calibration run was required to ensure no distortion occurred to the wires when the insert board, on which the wires are mounted, was removed from the calibrated bath and installed into the experimental test chamber.

C. INITIAL CALIBRATION

The initial calibration was conducted using the following equipment.

1. Rosemount Engineering Co. Model 913A calibration bath with Ethylene Glycol as the working fluid.
2. Rosemount Engineering Co. Model 923B power supply, controlling calibration bath temperature.
3. Rosemount Engineering Co. Model 920A commutating bridge, used to measure an resistance to 0.001Ω accuracy.
4. Rosemount Engineering Co. Model 162C S/N 985 Platinum Temperature Probe. Used to measure calibration bath temperature through the commutating bridge.
5. Hewlett Packard Data Acquisition System. Used to measure platinum wire resistance using a 4-wire ohm measurement technique.

1. Calibration Heating Bath

The present investigation was conducted using an externally heated calibration bath with ethylene glycol as the working fluid. This fluid was circulated by a centrifugal pump to ensure a uniform bulk temperature throughout the bath. Item (1) and item (2) are utilized.

2. Temperature Measurements

Temperature measurements for calibration were conducted using a high sensitivity commutating bridge to measure the resistance of a platinum resistance temperature probe. This platinum temperature probe had been previously calibrated to a standard that is traceable to the National Bureau of Standards.

3. Resistance Measurements

In calibrating the platinum wire the resistance of the wire was measured with the same Data Acquisition Unit Components as would be used in the experimental runs. This was to ensure the uncertainty of measured resistance would be the same as between the calibration run and experimental runs.

The Data Acquisition Unit Component used are:

1. HP3852A Control Unit
2. HP44701A Integrating Voltmeter card
3. HP44705A 20 channel Multiplexer card
4. HP300 series desk top computer
5. HP44713A 24 channel multiplexer with electronic cold junction for thermo couple measurements.

4. Calibration Procedure

By using the previously described components for measuring temperature and resistance, the following procedure was used to obtain the system's calibration data:

1. Set calibration bath controller for 35° C
2. Allow bath temperature to stabilize.
3. Carefully place Insert Board into bath liquid. EXTREME care must be taken to ensure that none of the wires are deformed or destroyed.
4. Allow insert board to come to thermal equilibrium with the bath, this takes approximately five minutes.
5. Take temperature reading with platinum wire temperature probe and commutator bridge, and resistance measurement of wires with data acquisition unit.
6. Remove insert board, and set bath temperature controller for a 5° C increase.
7. Repeat step 2 thru 6 until an 90° C reading has been achieved.

8. Activate External Cooling system.
9. With temperature control setting decreasing at 5° C intervals, repeat step 2 thru 6 until a 35° C reading has been achieved.

D. IN PLACE CALIBRATION

To ensure that the calibration curve of platinum wire 1 thru 5 are reliable, an in place calibration run was performed on the wires. This calibration procedure was performed before any experimental runs were conducted, and after the last experimental run was completed to detect any changes in calibration due to wire deformation or aging.

The equipment utilized for the inplace calibration was the same Data Acquisition equipment used for the resistance measurements of the Bath Calibration runs with two additions.

1. HP44713A 24 Channel Multiplexer with electronic cold junction.
2. Four type T thermocouples.

The thermocouples are now utilized, instead of the platinum resistance temperature probe, for measuring fluid bulk temperature. The uncertainty associated with the thermocouples is 0.4°C as compared to the platinum resistance temperature probe used as a standard. Figure 30 shows the thermocouples uncertainty compared to the platinum resistance temperature probe.

1. Inplace Calibration Procedure.

The following procedure is used for inplace calibration of the platinum wires:

1. Ensure Data Acquisition system is wired for 4-wire ohm measurements.
2. Turn on Data Acquisition system and allow one hour of warm-up time.
3. Load Calibration Acquisition Program into the HP-300 series Computer. See Appendix D for program listing.
4. Set power supply to bulk heaters to 20volts and 1.8 amps.
5. Start Acquisition program. The acquisition program will measure the resistance of each platinum wire, and measure the temperature output of each thermocouple at a 10 minute interval.
6. Allow acquisition program to run until bulk fluid has reached Saturation temperature of 56° C.

E. CALIBRATION RESULTS

1. Platinum Wire 1

From Figure 31 the importance of conducting an in place calibration prior to any experimental runs becomes obvious. wire 1's Bath calibration data has been con-

siderably altered while it was being inserted into the test chamber. The initial in place calibration data was used for the experimental runs calibration curve. The resulting calibration was:

$$T_1 = 53.902 \times R_1 - 254.470 (^{\circ}\text{C})$$

From Figure 32 it can be seen that the post calibration curve matches well with the data acquisition curve.

2. Platinum Wire 2

From Figure 33, it is apparent that the initial in place calibration curve fairs in well with the calibration bath's decreasing data. The initial in place calibration data was used for the experimental runs calibration curve. The resulting calibration was:

$$T_2 = 53.666 \times R_2 - 253.009 (^{\circ}\text{C})$$

From Figure 34 it can be seen that the Post run calibration matches well with the Data Acquisition Calibration curve.

3. Platinum Wire 3

From Figure 35 it is apparent that wire 3's Bath calibration data has been altered between the calibration bath and insertion into the test chamber. The initial in place calibration data was used for the experimental runs calibration curve. The resulting calibration was:

$$T_3 = 53.141 \times R_3 - 252.729 (^{\circ}\text{C})$$

From Figure 36 it can be seen that the Post run calibration matches well with the Data Acquisition Calibration curve.

4. Platinum Wire 4

From Figure 37, it is apparent that the initial in place calibration curve fairs in well with the calibration bath's decreasing data. The initial in place calibration data was used for the experimental runs calibration curve. The resulting calibration was:

$$T_4 = 53.484 \times R_4 - 252.848 (^{\circ}\text{C})$$

Form Figure 38 it can be seen that the post run calibration matches well with the data acquisition calibration curve.

5. Platinum Wire 5

From Figure 39 it is clear to see the shift in calibration curves between the calibration bath data and initial inplace calibration data. The calibration data has been altered while it was being inserted into the test chamber obviously. The initial data calibration was used for the experimental run calibration curve. The resulting calibration was:

$$T_5 = 53.085 \times R_5 - 260.049 (^{\circ}\text{C})$$

From Figure 40 it can be further seen that a considerable error has been introduced into wire 5's calibration, an error of 3.7° C. This places an uncertainty value onto wire's 5 temperature data of at least 3.7° C, an unacceptable value.

THERMOCOUPLE CALIBRATION

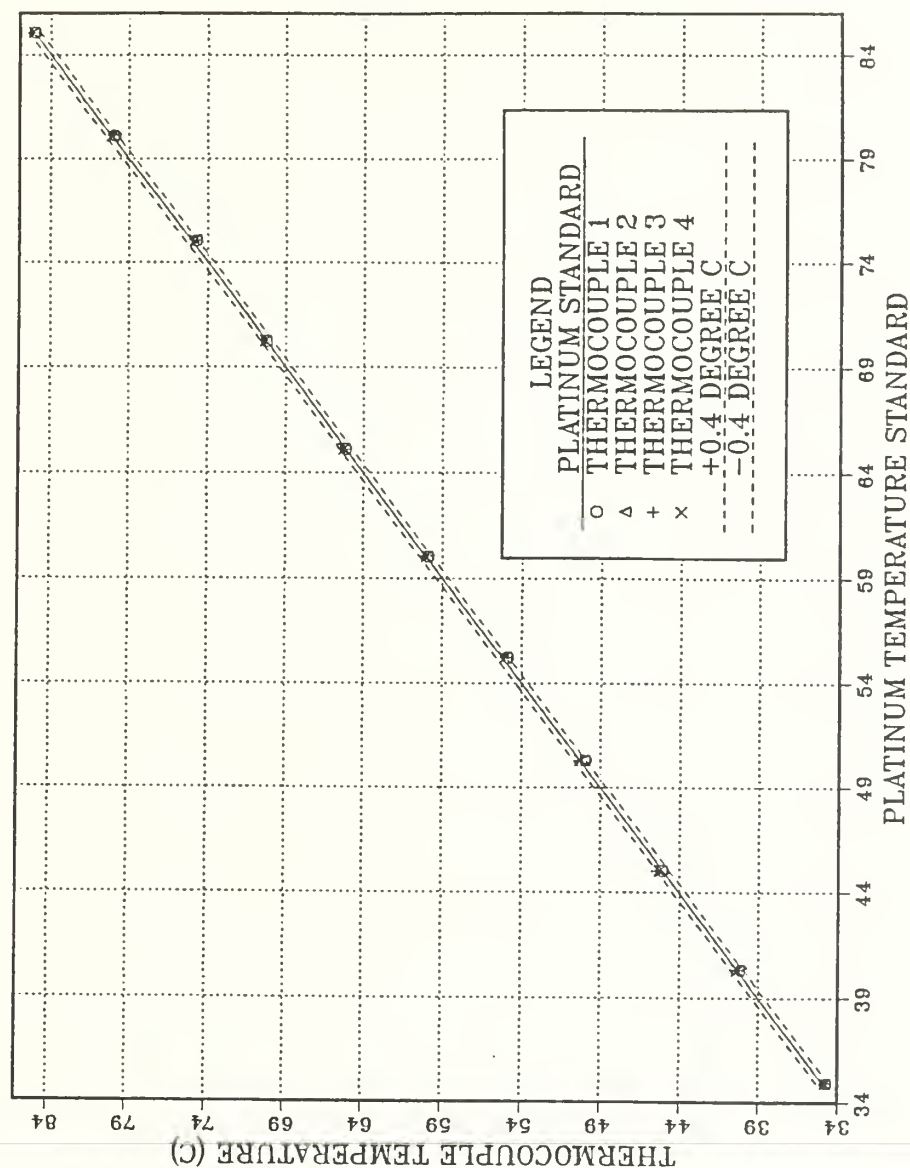


Figure 30. Thermocouple Uncertainty: Uncertainty of thermocouple's temperature measurements as compared to a platinum resistance temperature probe.

WIRE 1 CALIBRATION

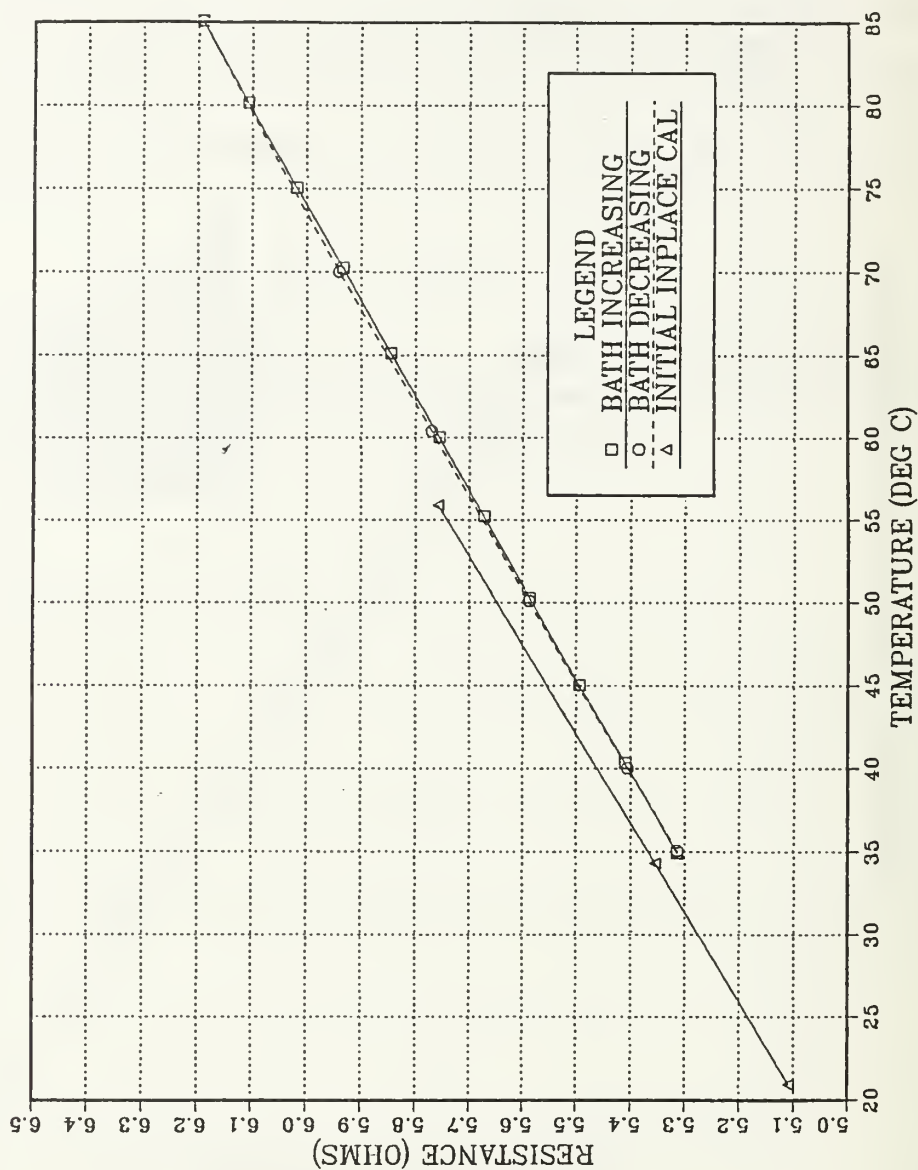


Figure 31. Calibration of Platinum Wire 1: Calibration curve of wire 1 of Calibration Bath Temperature Increasing, Calibration Bath Temperature Decreasing, and of the Initial in place calibration data.

WIRE 1 CALIBRATION

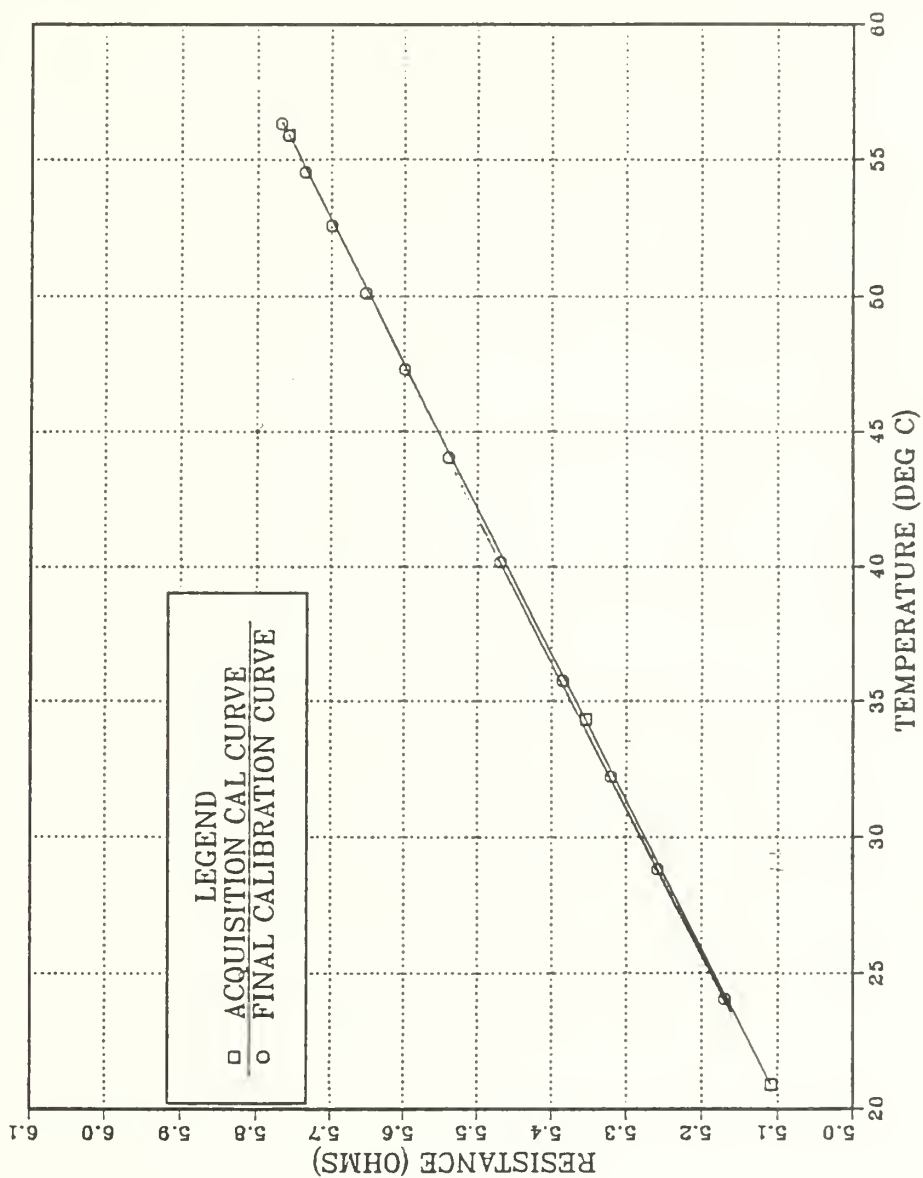


Figure 32. Calibration of Platinum Wire 1: Calibration curve of wire 1 of Initial in place calibration curve, and of Final in place calibration curve

WIRE 2 CALIBRATION

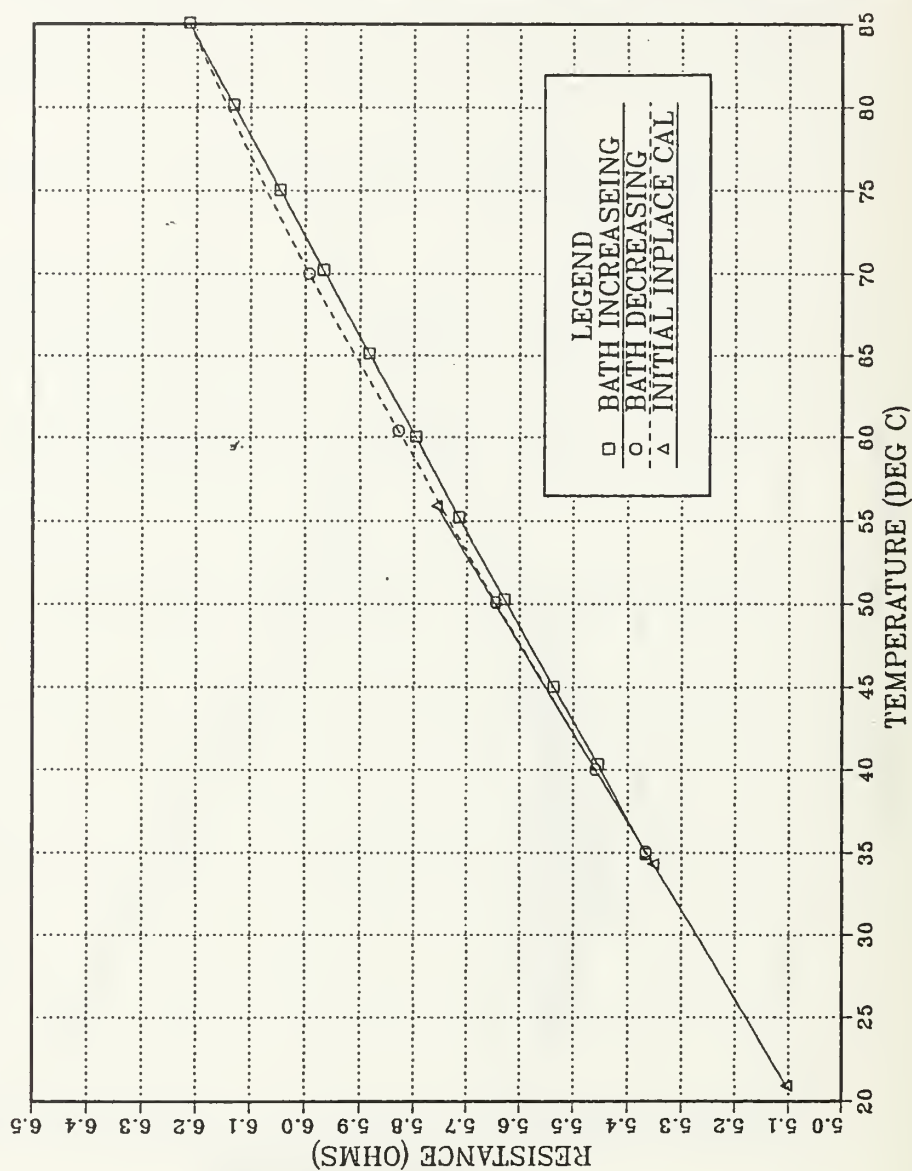


Figure 33. Calibration of Platinum Wire 2: Calibration curve of wire 2 of Calibration Bath Temperature Increasing, Calibration Bath Temperature Decreasing, and of the Initial in place calibration data.

WIRE 2 CALIBRATION

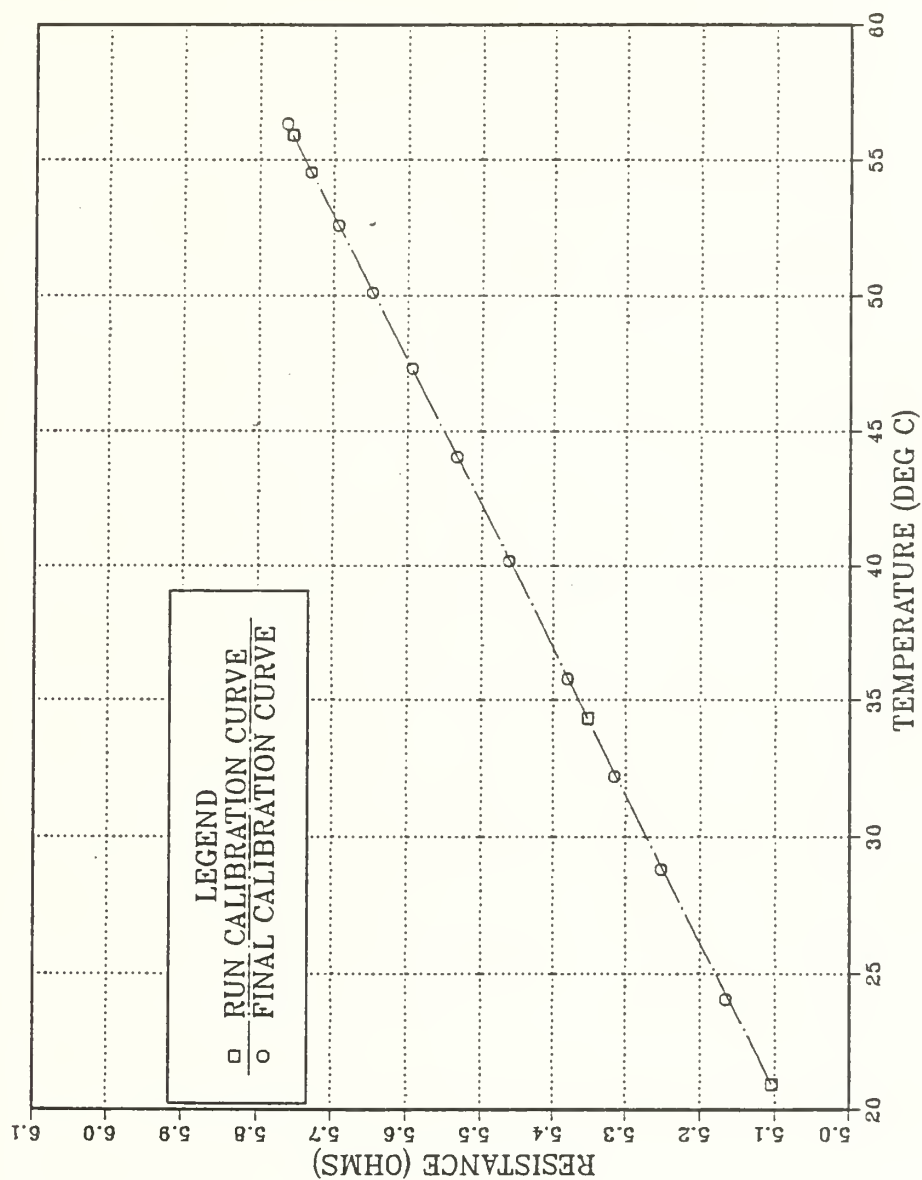


Figure 34. Calibration of Platinum Wire 2: Calibration curve of wire 2 of Initial in place calibration curve, and of Final in place calibration curve

WIRE 3 CALIBRATION

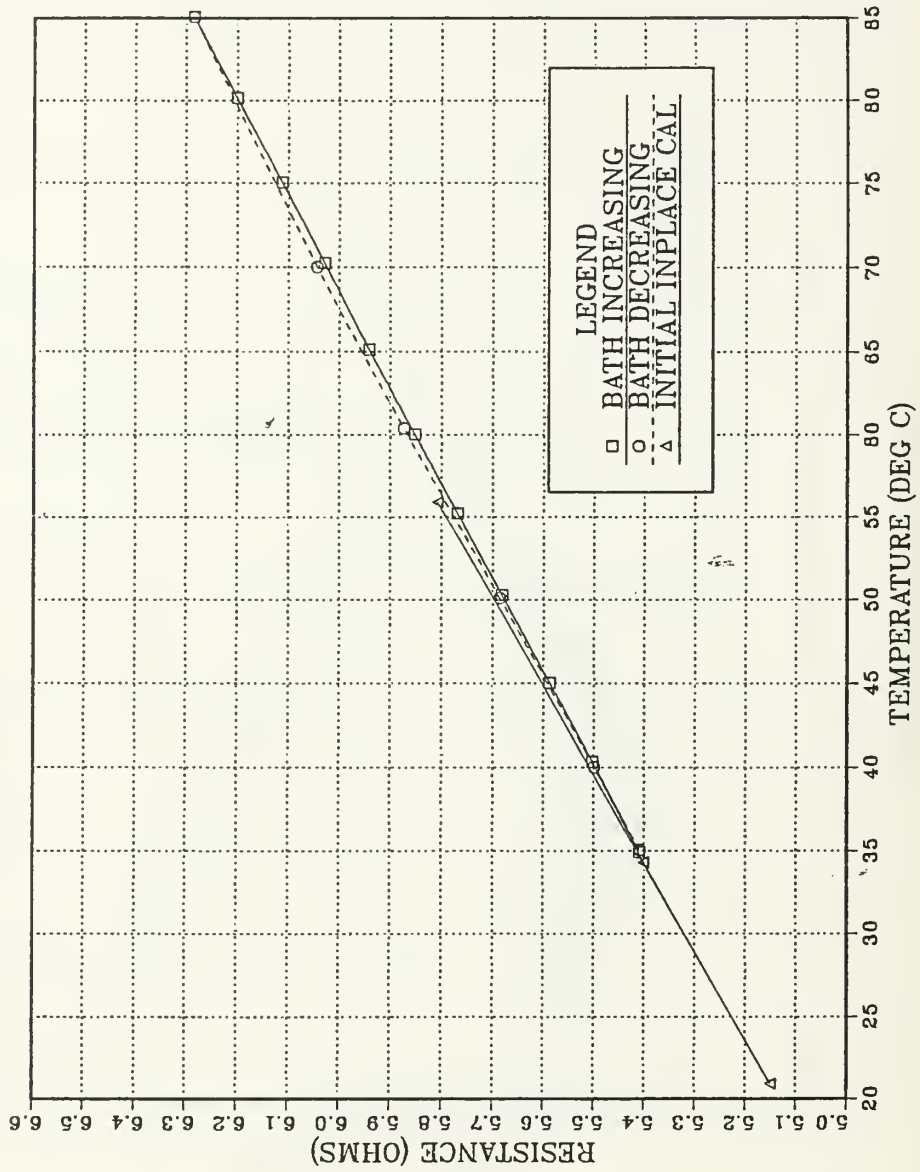


Figure 35. Calibration of Platinum Wire 3: Calibration curve of wire 3 of Calibration Bath Temperature Increasing, Calibration Bath Temperature Decreasing, and of the Initial in place calibration data.

WIRE 3 CALIBRATION

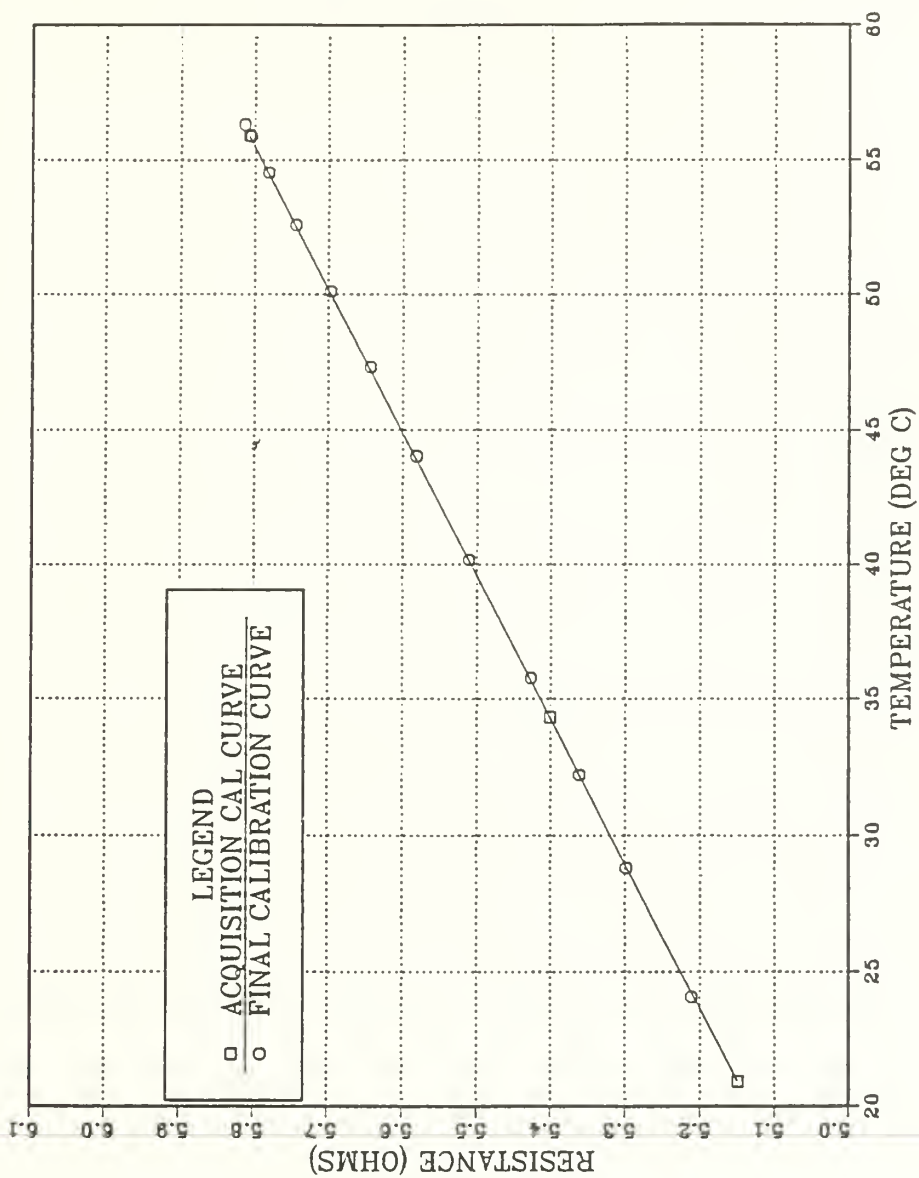


Figure 36. Calibration of Platinum Wire 3: Calibration curve of wire 3 of Initial in place calibration curve, and of Final in place calibration curve

WIRE 4 CALIBRATION

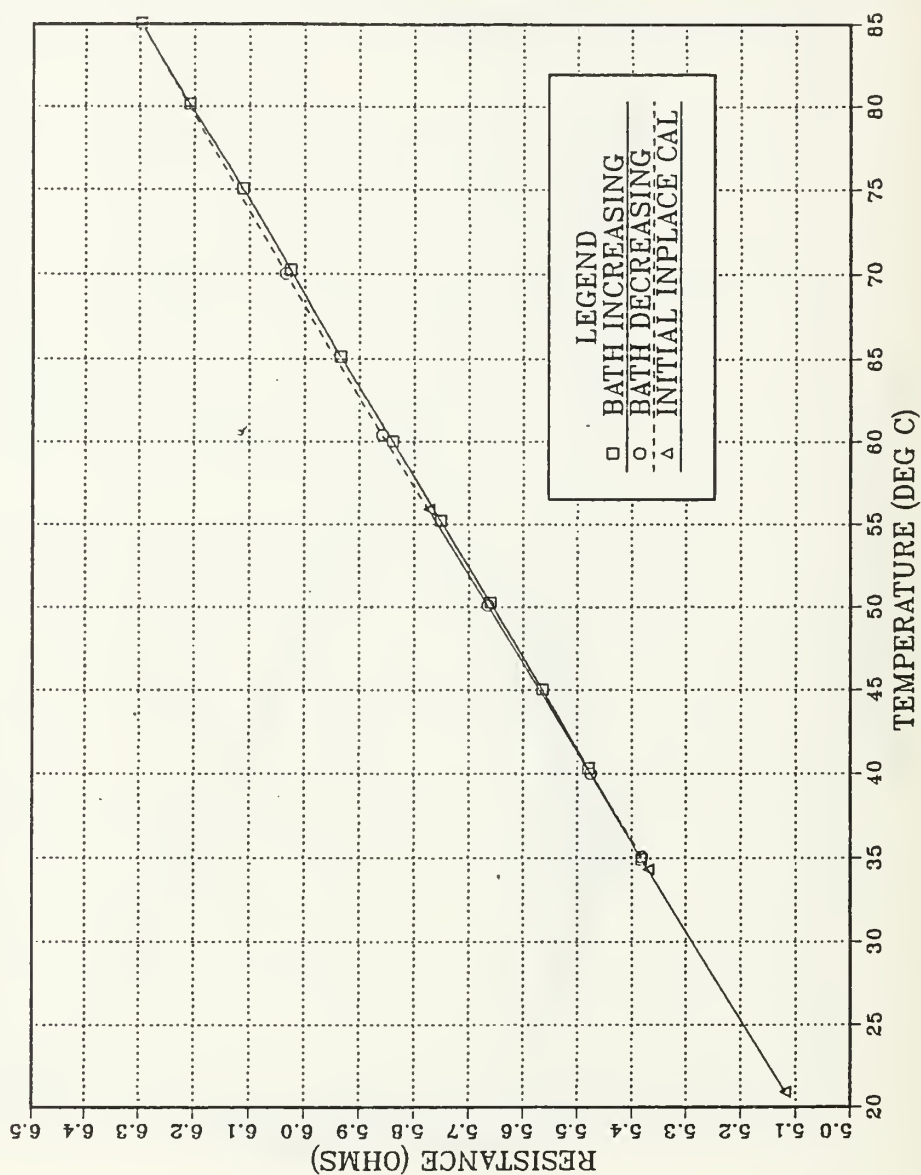


Figure 37. Calibration of Platinum Wire 4: Calibration curve of wire 4 of Calibration Bath Temperature Increasing, Calibration Bath Temperature Decreasing, and of the Initial in place calibration data.

WIRE 4 CALIBRATION

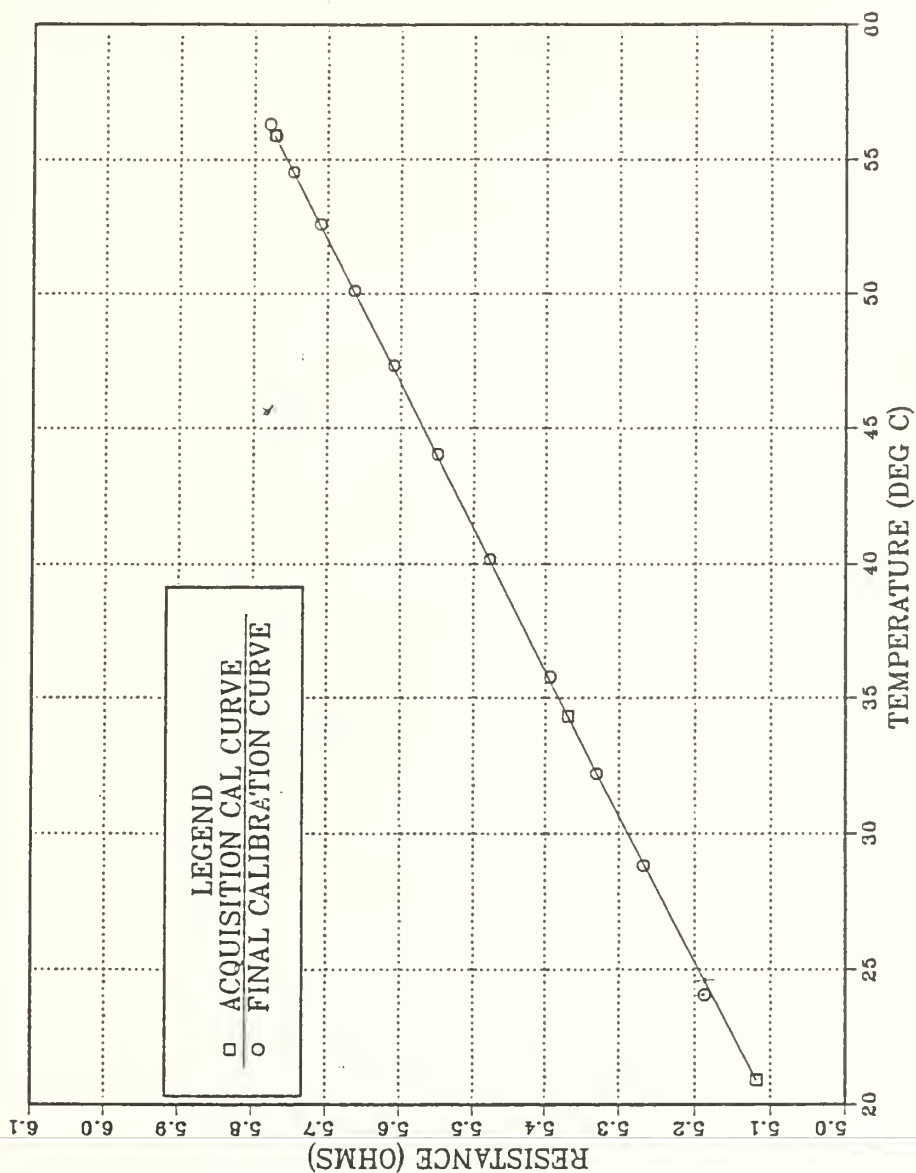


Figure 38. Calibration of Platinum Wire 4: Calibration curve of wire 4 of Initial in place calibration curve, and of Final in place calibration curve

WIRE 5 CALIBRATION

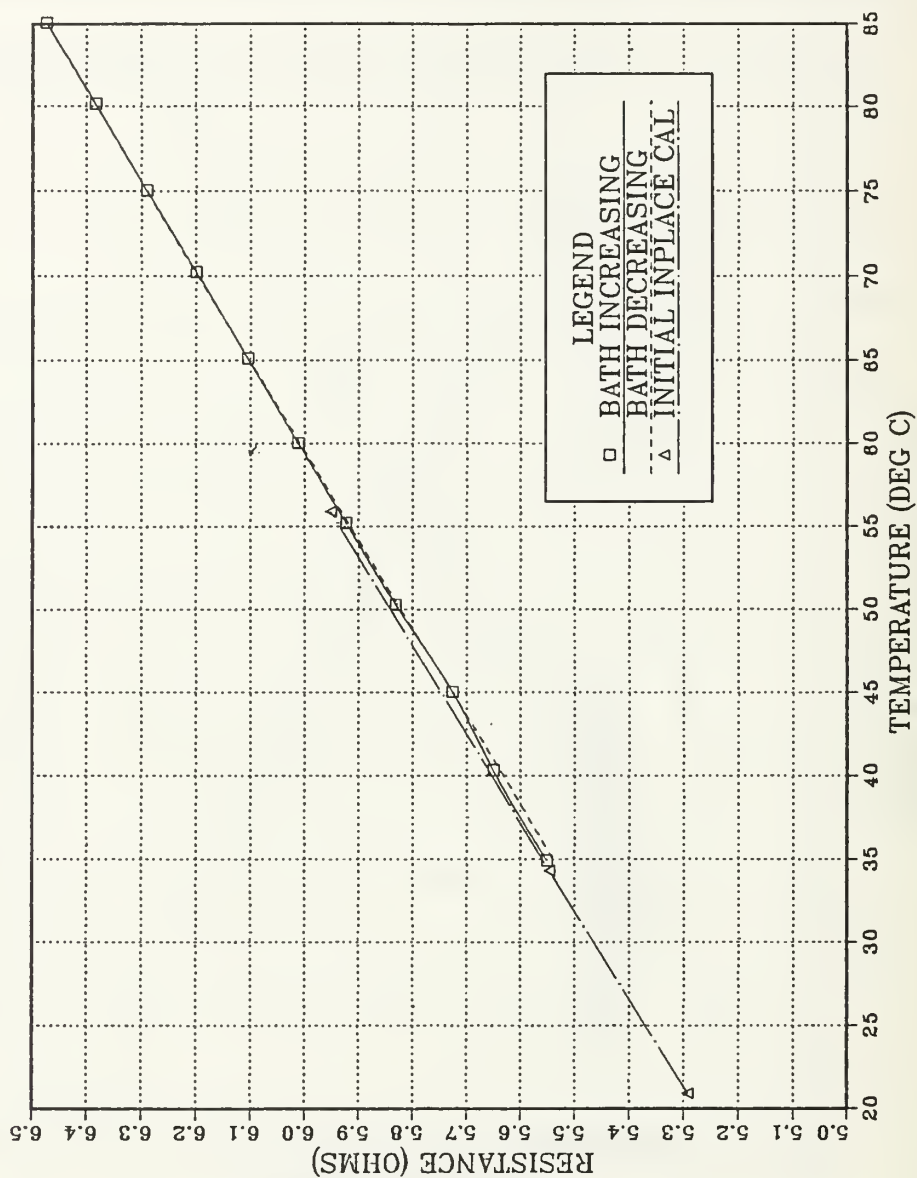


Figure 39. Calibration of Platinum Wire 5: Calibration curve of wire 5 of Calibration Bath Temperature Increasing, Calibration Bath Temperature Decreasing, and of the Initial in place calibration data.

WIRE 5 CALIBRATION

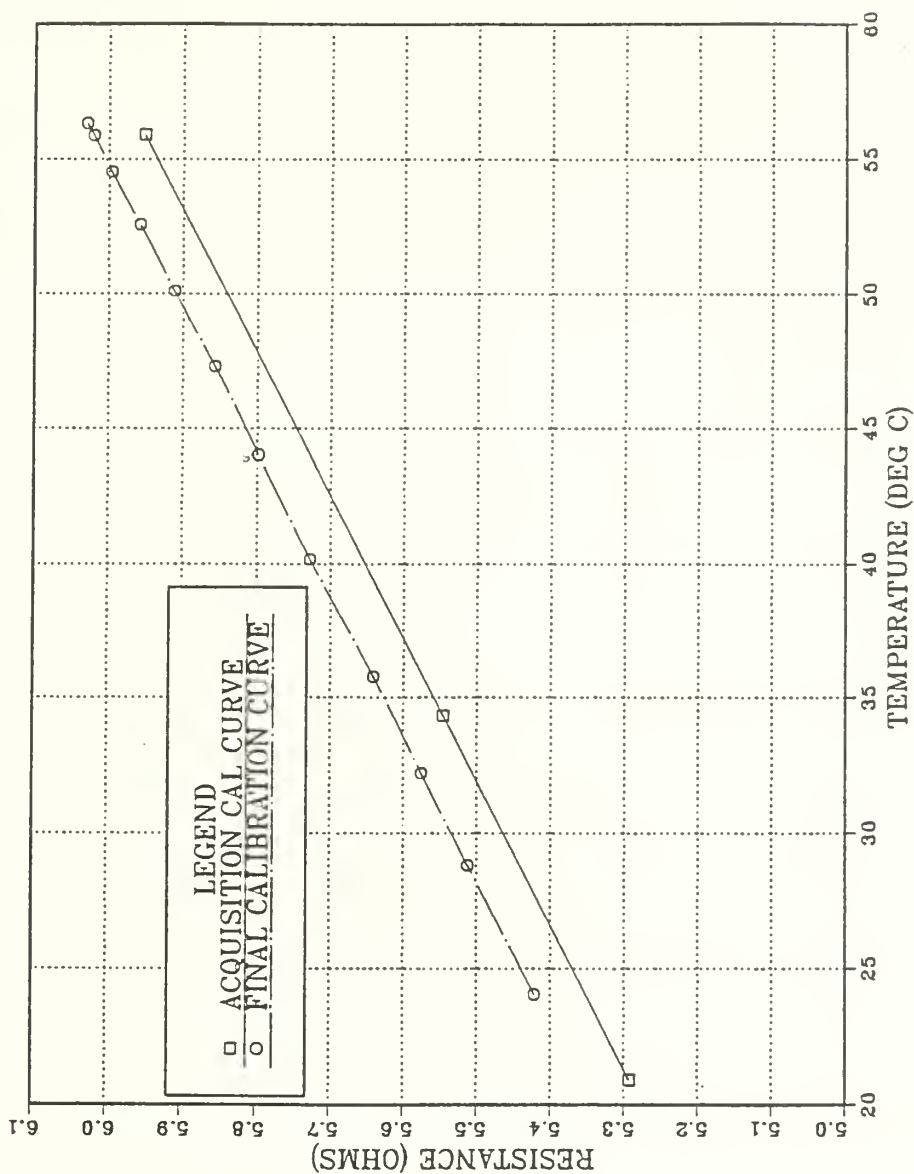


Figure 40. Calibration of Platinum Wire 5: Calibration curve of wire 5 of Initial in place calibration curve, and of Final in place calibration curve

F. SUMMARY

The following points were brought out during the calibration process.

1. The process of moving the platinum wires from the calibration bath and installing them into the test chamber resulted in a shift in the calibration curves.

2. The most probable cause of all the calibration shifts were the lead wires in the back of the insert board being pulled and adding an additional tension onto the platinum wires, thereby stretching them. The fact that the calibration curves consistently shifted to an increase in resistance supports this theory.
3. The maximum difference observed between the Platinum Wire Temperature Probe and the Type T thermocouples were 0.4°C . Therefore, a temperature uncertainty for the in place calibration will be set at 0.4°C .
4. The differences between the wire's data acquisition calibration curve and the wire's final calibration curve did not exceed the thermocouples uncertainty in temperature.

APPENDIX B. SAMPLE CALCULATIONS

In these sample calculations the output value of wire 1 will be used.

A. DETERMINATION OF DERIVED VALUES

1. Determination of the Average Bulk Temperature

The average bulk temperature of the liquid was obtained by the arithmetic average of the four immersed thermocouple outputs.

$$\begin{aligned} T_{bulk} &= \frac{(T_1 + T_2 + T_3 + T_4)}{4.0} \\ &= \frac{(55.835 + 55.884 + 55.988 + 55.932)}{4.0} \\ &= 55.9098^\circ\text{C} \end{aligned}$$

2. Determination of Wire Current

The current flow through the platinum wire is obtained by measuring the voltage drop across a precision 2 ohm resistor.

$$\begin{aligned} I_{PtWire} &= \frac{V_{Res}}{R_{2\Omega}} \\ &= \frac{(0.74605\text{Volts})}{(1.9994\text{Ohm})} \\ &= 0.2381\text{Ohms} \end{aligned}$$

B. DETERMINATION OF PLATINUM WIRE RESISTANCE

the resistance value of the platinum wires are obtained by measuring the voltage drop across the desired wire and dividing it by the current flow through it.

$$\begin{aligned} R_{PtWire} &= \frac{V_{PtWire}}{I_{PtWire}} \\ &= \frac{(1.7233\text{Volts})}{(0.2831\text{Amps})} \\ &= 6.0874 \text{ Ohms} \end{aligned}$$

1. Determination of Wire Surface Temperature

The wire's surface temperature are obtained from the calibration curves shown in APPENDIX A, wire 1 will be shown as an example.

$$\begin{aligned}
T_{PtWire1} &= 53.902 \times R_{PtWire} - 254.470 \\
&= 53.902 \times 6.0874 - 254.470 \\
&= 73.356^\circ\text{C}
\end{aligned}$$

2. Determination of Input Power

The input power of the wires are determined from the current flow through the wire times the voltage drop across the wire.

$$\begin{aligned}
\text{Power}_1 &= V_{PtWire1} \times I_{PtWire1} \\
&= 1.7233\text{Volts} \times 0.2831\text{Ohms} \\
&= 0.48787\text{Watts}
\end{aligned}$$

3. Determination of Heat Flux

The heat flux dissipated by the platinum wire is determined from the inputted power divided by the wire's surface area.

$$\begin{aligned}
\text{Hflux}_1 &= \frac{\text{Power}_1}{A_1} \\
&= \frac{(0.48787\text{Watts})}{1.5585\text{E-}5\text{m}^2} \\
&= 31,303.44\text{Watts/m}^2
\end{aligned}$$

where,

$$\begin{aligned}
A_1 &= \pi \times D_1 \times L_1 \\
&= \pi \times 5\text{E-}5 \text{ m} \times 0.09922\text{m} \\
&= 1.5585\text{E-}5\text{m}^2
\end{aligned}$$

C. DETERMINATION OF FLUID PROPERTIES

1. Film Temperature

The film temperature is the arithmetic average of bulk fluid temperature, and the wire's surface temperature.

$$\begin{aligned}
T_{film} &= \frac{(T_{bulk} + T_{PtWire})}{2.0} \\
&= \frac{(54.0^\circ\text{C} + 58.0^\circ\text{C})}{2.0} \\
&= 56.0^\circ\text{C}
\end{aligned}$$

2. Thermal Conductivity

From Figure 5 of the 3M Corporation Fluorinert Product Manual [Ref. 3 : p. 15], the thermal conductivity has been determined to be:

$$k = \frac{(0.6033 - 0.00115 \times T_{film})}{10.}$$
$$= 0.05389 \text{ Watts/m}^\circ\text{C}$$

at $T_{film} = 56^\circ\text{C}$

3. Liquid Density

Using the expressions in Table 4B and the constants presented in Table 4C of the 3M Corporation Product Manual,[Ref. 3: p.10], the liquid density has been determined to be:

$$\rho_l = (1.740 - 0.00261 \times T_{film}) \times 1000$$
$$= 1,593.8 \text{ kg/m}^3$$

at $T_{film} = 56^\circ\text{C}$

4. Kinematic Viscosity

Using Figure 3 in the 3M Corporation Product Manual, [Ref. 3: p.13] and determining an exponential curve fit valid from 0°C to 90°C yields:

$$v = A \exp\left(\frac{B}{T_{film} + 273.15^\circ\text{C}}\right)$$

$$A = 1.203952\text{E} - 8 \text{ m}^2/\text{s}$$

$$B = 1,058.4109^\circ\text{K}$$

at $T_{film} = 56^\circ\text{C}$

$$v = 3.000\text{E} - 7 \text{ m}^2/\text{s}$$

5. Specific Heat

From Figure 4 of the 3M Corporation Fluorinert Product Manual, [Ref. 3 : p.14], the specific heat has been determined to be:

$$C_p = (0.241111 + 3.70374\text{E} - 4 \times T_{film}) \times 4186$$
$$= 1,096.1 \text{ J/kg}^\circ\text{C}$$

at $T_{film} = 56^\circ\text{C}$

6. Thermal Expansion Coefficient

Using the expression in Table 4B and the constants presented in Table 4C of the 3M Corporation Product Manual, [Ref. 3: p.10], the thermal expansion coefficient has been determined to be:

$$\begin{aligned}\beta &= \frac{0.00261}{(1.740 - 0.00261 \times T_{film})} \\ &= 0.00164 \text{ } 1/^{\circ}\text{C}\end{aligned}$$

at $T_{film} = 56^{\circ}\text{C}$

7. Thermal Diffusivity

Is determined to be at $T_{film} = 56^{\circ}\text{C}$

$$\begin{aligned}\alpha &= \frac{k}{\rho \times C_p} \\ &= 3.0848\text{E} - 8 \text{ m}^2/\text{s}\end{aligned}$$

8. Prandlt Number

Prandlt Number is determined to be at $T_{film} = 56^{\circ}\text{C}$

$$\begin{aligned}\text{Pr} &= \frac{\nu}{\alpha} \\ &= 9.725\end{aligned}$$

APPENDIX C. UNCERTAINTY ANALYSIS

A. UNCERTAINTY IN SURFACE AREA

$$\omega_D = 0.003 \text{ mm}$$

$$\omega_L = 0.8 \text{ mm}$$

$$A = \pi D L$$

where:

D = Wire Diameter

L = Length of platinum wire

A = Surface Area of platinum wire

$$\frac{\partial A}{\partial D} = (\pi L)$$

$$\frac{\partial A}{\partial L} = (\pi D)$$

Therefore,

$$\omega_A = [(\pi L \omega_D)^2 + (\pi D \omega_L)^2]^{1/2}$$

$$\begin{aligned} \frac{\omega_A}{A} &= \left[\left(\frac{\omega_D}{D} \right)^2 + \left(\frac{\omega_L}{L} \right)^2 \right]^{1/2} \\ &= \left[\left(\frac{0.003}{0.05} \right)^2 + \left(\frac{0.8}{99.22} \right)^2 \right]^{1/2} \end{aligned}$$

$$\frac{\omega_A}{A} = 0.061 \text{ or } 6.1\%$$

$$\omega_A = 9.43529\text{E} - 7 \text{ m}^2$$

B. UNCERTAINTY IN POWER

$$\omega_{V,2\Omega} = 0.008\% + 8\mu V \quad [\text{Ref 13, pg.587}]$$

$$\omega_{V,PtWire} = 0.008\% + 8\mu V \quad [\text{Ref 13, pg.587}]$$

$$\omega_{R,2\Omega} = \pm 0.001\Omega \text{ max value}$$

$$Q = V_{PtWire} \times I_{PtWire}$$

$$= V_{PtWire} \times \frac{V_{2\Omega}}{R_{2\Omega}}$$

$$\frac{\partial Q}{\partial V_{PtWire}} = \frac{V_{2\Omega}}{R_{2\Omega}}$$

$$\frac{\partial Q}{\partial V_{2\Omega}} = \frac{V_{PtWire}}{R_{2\Omega}}$$

$$\frac{\partial Q}{\partial R_{2\Omega}} = -V_{PtWire} \times \frac{V_{2\Omega}}{R_{2\Omega}^2}$$

$$\omega_Q = \left[\left(\frac{V_{2\Omega}}{R_{2\Omega}} \times \omega_{V,PtWire} \right)^2 + \left(\frac{V_{PtWire}}{R_{2\Omega}} \times \omega_{V,2\Omega} \right)^2 + \left(-V_{PtWire} \times \frac{V_{2\Omega}}{R_{2\Omega}^2} \times \omega_{R,2\Omega} \right)^2 \right]^{1/2}$$

$$\frac{\omega_Q}{Q} = \left[\left(\frac{\omega_{V,PtWire}}{V_{PtWire}} \right)^2 + \left(\frac{\omega_{V,2\Omega}}{V_{2\Omega}} \right)^2 + \left(\frac{\omega_{R,2\Omega}}{R_{2\Omega}} \right)^2 \right]^{1/2}$$

The worst case of uncertainty will occur when the voltages measured for V_{PtWire} and $V_{2\Omega}$ are small, less than 0.3 Volts.

$$\frac{\omega_Q}{Q} = \left[(0.008\% + 0.0027\%)^2 + (0.008\% + 0.0027\%)^2 + \left(\frac{0.001}{1.9994 \times 100} \% \right)^2 \right]^{1/2}$$

$$= 0.0524\% \text{ or } 5.2384E-4$$

C. UNCERTAINTY IN HEAT FLUX

$$q = \frac{Q}{A}$$

$$\frac{\partial q}{\partial Q} = \frac{1}{A}$$

$$\frac{\partial q}{\partial A} = \frac{-Q}{A^2}$$

$$\omega_q = \left[\left(\frac{-Q}{A^2} \omega_A \right)^2 + \left(\frac{1}{A} \omega_A \right)^2 \right]^{1/2}$$

$$\frac{\omega_q}{q} = \left[\left(\frac{\omega_A}{A} \right)^2 + \left(\frac{\omega_q}{Q} \right)^2 \right]^{1/2}$$

$$= [(0.061)^2 + (5.2384E-4)^2]^{1/2}$$

$$= 6.1002E-2 \text{ or } \% 6.1$$

D. UNCERTAINTY IN TEMPERATURE

The uncertainty in the thermocouple measurements (ω_{TC}) is determined by the uncertainty in the platinum wire temperature probe ($\omega_{PtProbe}$) and the error in the thermocouple's in matching the probe temperature ($\omega_{\Delta TC}$).

$$\omega_{TC} = [(\omega_{PtProbe})^2 + (\omega_{\Delta TC})^2]^{1/2}$$

$$= 0.4001^\circ\text{C}$$

E. UNCERTAINTY OF WIRE SURFACE TEMPERATURE

From the calibration formula

$$\omega_\epsilon = 0.1 \frac{^\circ\text{C}}{\Omega}$$

$$\omega_{To} = 0.4001^\circ\text{C}$$

$$\begin{aligned}
T_{surf} &= \varepsilon R_{PtWire} + T_0 \\
&= \varepsilon V_{PtWire} \frac{R_{2\Omega}}{V_{2\Omega}} + T_0 + \delta T
\end{aligned}$$

Where:

ε = slope of calibration curve

T_0 = axis intercept for $R = 0$

V_{PtWire} = Voltage drop across Platinum Wire

$R_{2\Omega}$ = Resistance of in series Resistor

$V_{2\Omega}$ = Voltage drop across series Resistor

δT = Difference between Data Acquisition and Final Calibration for a particular data po

$$\frac{\partial T_{surf}}{\partial \varepsilon} = \frac{V_{PtWire}}{V_{2\Omega}} R_{2\Omega}$$

$$\frac{\partial T_{surf}}{\partial T_0} = 1$$

$$\frac{\partial T_{surf}}{\partial \delta T} = 1$$

$$\frac{\partial T_{surf}}{\partial V_{PtWire}} = \varepsilon \frac{R_{2\Omega}}{V_{2\Omega}}$$

$$\frac{\partial T_{surf}}{\partial R_{2\Omega}} = \varepsilon \frac{V_{PtWire}}{V_{2\Omega}}$$

$$\frac{\partial T_{surf}}{\partial V_{2\Omega}} = -\varepsilon V_{PtWire} \frac{R_{2\Omega}}{V_{2\Omega}^2}$$

$$\omega_{Tsurf} = \left[\left(\frac{V_{PtWire} R_{2\Omega}}{V_{2\Omega}} \omega_{\epsilon} \right)^2 + (1 \omega_{To})^2 + \left(\epsilon \frac{R_{2\Omega}}{V_{2\Omega}} \omega_{V,PtWire} \right)^2 + \left(\epsilon \frac{V_{PtWire}}{V_{2\Omega}} \omega_{2\Omega} \right)^2 \right] \\ \left[\left(-\epsilon V_{PtWire} \frac{R_{2\Omega}}{V_{2\Omega}^2} \omega_{V,2\Omega} \right)^2 + (1 \omega_{\delta T})^2 \right]^{1/2}$$

Using data from Wire 1 at the following point,

$$V_{PtWire} = 0.71673 \text{ Volts}$$

$$V_{2\Omega} = 0.24529 \text{ Volts}$$

$$R_{2\Omega} = 1.9994 \text{ Ohms for wire 1}$$

$$\epsilon_{wire1} = 53.902^\circ\text{C}/\Omega$$

$$\delta T = 0.02^\circ\text{C}$$

This results in an uncertainty in temperature of,

$$\omega_{Tsurf,wire1} = 0.854^\circ\text{C}$$

APPENDIX D. DATA ACQUISITION PROGRAMS USED

A. PLATINUM WIRE RESISTANCE CALIBRATION PROGRAM

The following program was used to obtain the Resistance value's for the platinum wire specimans used in chapter 2. This program is written in HP basic language for use with controlling the HP-3852A Data Acquisition unit.

```
10 DIM Ohms(0:61)
20 OUTPUT 709;"INTEGER I"
30 OUTPUT 709;"RST 000"
40 OUTPUT 709;"USE 000"
50 OUTPUT 709;"CONF OHMF"
60 OUTPUT 709;"NPLC 1.0"
70 OUTPUT 709;"NRDGS 62"
80 OUTPUT 709;"DELAY 0.1"
90 OUTPUT 709;"RANGE 10"
100 OUTPUT 709;"I = 99"
110 OUTPUT 709;"I = 1 + I"
120 OUTPUT 709;"MEAS OHMF,I"
130 ENTER 709;Ohms(*)
140 Alo=1.E+30
150 J=1+J
160 Ahi=1.E-30
170 A=0.
180 FOR K=1 TO 60
190 A=A+Ohms(K)
200 IF Ohms(K)<Alo THEN
210 Alo=Ohms(K)
220 END IF
230 IF Ohms(K)>Ahi THEN
240 Ahi=Ohms(K)
250 END IF
260 NEXT K
270 B=A/60.
280 PRINT "WIRE SAMPLE ";J
290 PRINT "60 RESISTANCE AVERAGE IS ";B
300 PRINT "LO RESISTANCE MEASURED IS ";Alo
310 PRINT "HI RESISTANCE MEASURED IS ";Ahi
320 IF J=5 THEN
330 GOTO 360
340 END IF
350 GOTO 110
360 GOTO 370
370 DIM Temps(0:61)
380 K=0.
390 OUTPUT 709;"RST 000"
400 OUTPUT 709;"USE 000"
410 OUTPUT 709;"INTEGER I"
```

```

420 OUTPUT 709;"CONF TEMPT"
430 OUTPUT 709;"NPLC 1.0"
440 OUTPUT 709;"NRDGS 62"
450 OUTPUT 709;"DELAY 0.1"
460 OUTPUT 709;"RANGE AUTO"
470 OUTPUT 709;"I=299"
480 OUTPUT 709;"I=I+1"
490 OUTPUT 709;"MEAS TEMPT,I"
500 ENTER 709;Tems(*)
510 K=K+1
520 A=0.
530 FOR L=1 TO 60
540 A=A+Tems(L)
550 NEXT L
560 Temp=A/60.
570 PRINT "THERMOCOUPLE";K;"TEMPERATURE";Temp
580 IF K=4 THEN
590 GOTO 620
600 END IF
610 GOTO 480
620 END

```

B. MAIN DATA ACQUISITION PROGRAM

The following program was used to obtain the Temperature value's for the platinum wire specimans used in chapter 3. This program is written in HP basic language for use with controlling the HP-3852A Data Acquisition unit.

```
10    DIM Temps(0:16),Tk(1:7),Tt(1:100),Flux(1:100),Tb(100)
20    L=0
30    J=0
40    L=L+1
50    IF L=81 THEN
60    GOTO 1450
70    END IF
80    OUTPUT 709;"RST 000"
90    OUTPUT 709;"USE 000"
100   OUTPUT 709;"INTEGER I"
110   OUTPUT 709;"CONF TEMPT"
120   OUTPUT 709;"NPLC 1.0"
130   OUTPUT 709;"NRDGS 17"
140   OUTPUT 709;"DELAY 0.1"
150   OUTPUT 709;"RANGE AUTO"
160   OUTPUT 709;"I=299"
170   OUTPUT 709;"I=I+1"
180   OUTPUT 709;"MEAS TEMPT,I"
190   ENTER 709;Temps(*)
200   J=J+1
210   A=0.
220   FOR K=1 TO 15
230   A=A+Temps(K)
240   NEXT K
250   Tk(J)=A/15.
260   IF J=7 THEN
270   GOTO 300
280   END IF
290   GOTO 170
300   DIM Volts(0:11),Vk(1:10)
310   J=0.
320   Ct=0.
330   OUTPUT 709;"RST 000"
340   OUTPUT 709;"USE 000"
350   OUTPUT 709;"INTEGER I"
360   OUTPUT 709;"CONF DCV"
370   OUTPUT 709;"NPLC 1.0"
380   OUTPUT 709;"NRDGS 12"
390   OUTPUT 709;"DELAY 0.1"
400   OUTPUT 709;"RANGE AUTO"
410   OUTPUT 709;"I=99"
420   OUTPUT 709;"I=I+1"
430   OUTPUT 709;"MEAS DCV,I"
440   ENTER 709;Volts(*)
450   J=J+1
```

```

460 IF J=5 THEN
470 GOTO 420
480 END IF
490 Ct=Ct+1
500 A=0.
510 FOR K=1 TO 10
520 A=A+Volts(K)
530 NEXT K
540 Vk(Ct)=A/10.
550 IF J=6 THEN
560 GOTO 590
570 END IF
580 GOTO 420
590 DIM Voltw(0:11)
600 J=0.
610 Ct=5.
620 OUTPUT 709;"RST 000"
630 OUTPUT 709;"USE 000"
640 OUTPUT 709;"INTEGER I"
650 OUTPUT 709;"CONF DCV"
660 OUTPUT 709;"NPLC 1.0"
670 OUTPUT 709;"NRDGS 12"
680 OUTPUT 709;"DELAY 0.1"
690 OUTPUT 709;"RANGE AUTO"
700 OUTPUT 709;"I=109"
710 OUTPUT 709;"I=I+1"
720 OUTPUT 709;"MEAS DCV,I"
730 ENTER 709;Voltw(*)
740 J=J+1
750 IF J=5 THEN
760 GOTO 710
770 END IF
780 Ct=Ct+1
790 A=0.
800 FOR K=1 TO 10
810 A=A+Voltw(K)
820 NEXT K
830 Vk(Ct)=A/10.
840 IF J=6 THEN
850 GOTO 880
860 END IF
870 GOTO 710
880 Bt=(Tk(1)+Tk(2)+Tk(3)+Tk(4))/4.
890 V1=Vk(6)
900 I1=Vk(1)/1.9994
910 V2=Vk(7)
920 I2=Vk(2)/2.0076
930 V3=Vk(8)
940 I3=Vk(3)/1.9997
950 V4=Vk(9)
960 I4=Vk(4)/2.0018
970 V5=Vk(10)
980 I5=Vk(5)/2.0025

```

```

990  P1=I1*V1
1000 P2=I2*V2
1010 P3=I3*V3
1020 P4=I4*V4
1030 P5=I5*V5
1040 R1=V1/I1
1050 R2=V2/I2
1060 !R3=V3/I3
1070 !R4=V4/I4
1080 !R5=V5/I5
1090 Flux1=P1/1.5585284E-5
1100 Flux2=P2/1.5585284E-5
1110 Flux3=P3/1.5710005E-5
1120 Flux4=P4/1.5460563E-5
1130 Flux5=P5/1.5710005E-5
1140 T1=(53.902123*R1)-254.46995
1150 T2=(53.666456*R2)-253.00959
1160 T3=(53.141047*R3)-252.729131
1170 T4=(53.483646*R4)-252.848797
1180 T5=(53.085508*R5)-260.04883
1190 Tc=(Tk(5)+Tk(6))/2.
1200 PRINT " TEMPERATURES"
1210 PRINT " AMBIENT AIR BULK FLUID CONDENSOR SURFACE"
1220 PRINT Tk(7),Bt,Tc
1230 PRINT " " " ,L
1240 PRINT "WIRE TEMPERATURE CURRENT VOLTS "
1250 !PRINT " (AMPS) (VOLTS) (DEGREE C) "
1260 PRINT "1",T1,I1,V1
1270 PRINT "2",T2,I2,V2
1280 !PRINT "3",T3,I3,V3
1290 !PRINT "4",T4,I4,V4
1300 !PRINT "5",T5,I5,V5
1310 PRINT " HEAT FLUX POWER RESISTANCE "
1320 !PRINT " (WATTS) (OHMS) (WATTS/M2)"
1330 PRINT "1",Flux1,P1,R1
1340 PRINT "2",Flux2,P2,R2
1350 !PRINT "3",FLUX3,P3,R3
1360 !PRINT "4",Flux4,P4,R4
1370 !PRINT "5",Flux5,P5,R5
1380 PRINT " "
1390 Tt(L)=T1
1400 Tb(L)=Bt
1410 Flux(L)=Flux1
1420 WAIT 100
1430 GOTO 30
1440 GOTO 1530
1450 M=1
1460 PRINT " WIRE TEMP HEAT FLUX BULK TEMP"
1470 IF M=3 THEN
1480 GOTO 1530
1490 END IF
1500 PRINT M,Tt(M),Flux(M),Tb(M)
1510 M=M+1
1520 GOTO 1470
1530 END

```

C. NUSSELT EVALUATION PROGRAM

The following program was used to obtain the Nusselt Number for the platinum wire specimens used in chapter 3. This program is written in Fortran language for use with controlling the IBM-3803 Main Frame Computer.

FILE: NUSSELT FORTRAN A1

```
      SUBROUTINE NUSSELT (X1,T1,M,Q)
C
C THIS SUBROUTINE WILL CALCULATE THE HEAT TRANSFER COEFFICIENT FOR THE
C DATA OBTAINED FROM THE EXPERIMENTAL RUNS BY USING THE CHURCHILL AND
C CHU CORRELATION
C
      DIMENSION X1(*),T1(*),Q(*)
      REAL*4 X1,T1,Q,K,NU,NUD
      OPEN(29,FILE='RALY',STATUS='UNKNOWN',FORM='FORMATTED')
C
C DIAMETER OF THE WIRE BEING ANALYSED IS NOMINALLY .05 MM
C
      D=5.0E-5
C
C GRAVITY TERM OF 9.81 M/S2
C
      G=9.81
C
      DO 100 I=1,M
C
C FILM TEMPERATURE OF THE PHYSICAL PROPERTIES
C
CCC   TF = (X1(I) + T1(I) + 56.0)/2.
      TF = (X1(I) + 2.*T1(I))/2.
C
C TEMPERATURE DIFFERENCE BETWEEN THE WIRE AND BULK FLUID
C
CCC   TD =(X1(I) - T1(I) + 56.0)
      TD = X1(I)
C
C THERMAL CONDUCTIVITY OF FLUID W/MK
C
      K = (0.6033 - 0.00115*TF)/10.
C
C BULK MODULUS OF THE FLUID 1/K
C
      BETA = 0.00261/(1.740 - 0.00261*TF)
C
C KINEMATIC VISCOSITY OF THE FLUID M2/S
C
      NU = 1.203952E-8 * EXP(1058.4109/(TF+273.15))
C
C SPECIFIC HEAT OF FLUID
C
      CP = (0.24111 + 3.70374E-4 * TF)*4186.00
C
C FLUID DENSITY KG/M3
C
      RHO = (1.740 - 0.00261*TF)*1000.0
C
```

```

C  THERMAL DIFFUSIVITY
C      ALFA = K/(RHO*CP)
C
C  PRANDLT NUMBER OF FLUID
C      PR = NU/ALFA
C
C  RAYLEIGH NUMBER OF FLUID  MUST BE  $10^{*-5} < RA < 10^{*12}$ 
C      RA = (G*BETA*TD*D**3.)/(NU*ALFA)
C      PRINT *, RA
C
C  NUSSELT NUMBER OF FLUID      NU=H*D/K
C
C      TERM = ((0.518*(RA**0.25))*(1+(0.559/PR)**0.6)**(-5./12.))**15
C      |+(0.1*RA**(1./3.))**15.))**15.))**15.))
C      NUD=2.0/(LOG(1.+ 2./TERM))
C
C  THERORICAL HEAT FLUX  WATTS/M2
C
C      Q(I) = K*NUD*TD/D
100  WRITE(29,500) TD,RA,NUD,PR,Q(I)
C
500  FORMAT (5(F12.4,2X))
      CLOSE (29)
      RETURN
      END

```

LIST OF REFERENCES

1. Bergles A.E., *Heat Transfer in Electronic and Microelectronic Equipment*, pp 3-60, Hemisphere Publishing Co. 1990.
2. Bergles A.E., and Kim C.J., "A Method to Reduce Temperature Overshoots in Immersion Cooling of Microelectronic Devices", paper presented at the 1987 ASME, JSME Thermal Engineering Joint Conference Honolulu, Hawaii, 1987.
3. 3M Corporation, *Flourinert Electronic Liquid Product Manual* Commercial Chemical Division: St. Paul Minnesota, 1987.
4. You S.M., Simon T.W., and Bar-Cohen A., "Experiments on Nucleate Boiling Heat Transfer with a Highly-Wetting Di-Electric Fluid: Effects of Pressure, Sub-Cooling, and Dissolved Gas Content," paper presented at the 1987 ASME, JSME Thermal Engineering Joint Conference, Honolulu, Hawaii, 1987.
5. You S.M., Simon T.W., and Bar-Cohen A., "Experiments on Boiling Incipience with a Highly-Wetting Dielectric Fluid: Effects of Pressure, Subcooling and Dissolved Gas Content," paper presented at the 1987 ASME, JSME Thermal Engineering Joint Conference, Honolulu, Hawaii, 1987.
6. You S.M., Simon T.W., Bar-Cohen A., and Tong W., "Experimental Investigation Nucleate Boiling Incipience with a Highly-Wetting Dielectric Fluid (R-113)," *International Journal of Heat and Mass Transfer*, v.33, No.1, pp.105-117, 1990.
7. Marto P.J., and Lepere V.J., "Pool Boiling Heat Transfer From Enhanced Surfaces to Dielectric Fluids," *ASME Journal of Heat Transfer*, v.104, pp.292-299, May 1982.
8. Maddox D.E., and Mudawar, I., "Single and Two-Phase Convective Heat Transfer from Smooth and Enhanced Microelectronic Heat Sources in a Rectangular Channel," *ASME Journal of Heat Transfer*, v.111, pp. 1045-1052.

9. Danielson R.D., Tousignant L. and Bar-Cohen A., "Saturated Pool Characteristics of Commercially Available Perfluorinated Inert Liquids," paper presented at the 1987 ASME, JSME Thermal Engineering Joint Conference, Honolulu, Hawaii, 1987.
10. Kuehn T.H. and Goldstein R.J., "Correlating Equations for Natural Convection Heat Transfer Between Horizontal Circular Cylinders," *International Journal of Heat and Mass Transfer*, v.19, pp.1127-1134, 1976.
11. Eren A.S., *Heat Transfer Enhancement due to Bubble Pumping in FC-72 Near Saturation Temperature*, Master's Thesis, Naval Postgraduate School, Monterey, California, March 1991.
12. Materials Electronic Products Corporation, *MELCOR FRIGICHIPS Product Manual*, Thermoelectric Cooler's Division: Trenton, New Jersey, 1985.
13. Hewlett Packard, *1991 Test and Measurement Catalog*, Pages 586 - 589.

INITIAL DISTRIBUTION LIST

	No. Copies
1. Defense Technical Information Center Cameron Station Alexandria, VA 22304-6145	2
2. Library, Code 52 Naval Postgraduate School Monterey, CA 93943-5002	2
3. Mechanical Engineering Curricular Office, Code ME Naval Postgraduate School Monterey, California 93940	1
4. Professor M.D. Kelleher, Code ME/Kk Naval Postgraduate School Monterey, California 93943-5000	2
5. Professor Y. Joshi, Code ME/Ji Naval Postgraduate School Monterey, California 93943-5000	1
6. Naval Weapons Support Center Code 6042 Crane, Indiana 47522	1
7. LtJg Ali Sükrü Eren Harzem Sok 5/3, 80650 Celiktepe, Istanbul, Turkey	1
8. LT R.A. Egger 4830 Rocky River Drive Cleveland, Ohio 44135	2

Thesis

E2655 Egger

c.1 Enhancement of boiling
heat transfer in
di-electric fluids.

Thesis

E2655 Egger

c.1 Enhancement of boiling
heat transfer in
di-electric fluids.

DODLEY KNOX LIBRARY



3 2768 00034147 3